

**Application of GIS and Remote Sensing Techniques for the Estimation of
Soil Erosion- Case Study: Soan River Catchment**



By

Muhammad Usman Ejaz

(MS WRE&M 2019, 00000319619)

Department of Water Resources Engineering and Management

NUST Institute of Civil Engineering

School of Civil and Environmental Engineering

National University of Sciences and Technology

Sector H-12, Islamabad, Pakistan

(2023)

**Application of GIS and Remote Sensing Techniques for the Estimation of
Soil Erosion- Case Study: Soan River Catchment**



By

Muhammad Usman Ejaz

(Registration No: MS WRE&M 2019, 00000319619)

A thesis submitted to the National University of Sciences and Technology,
Islamabad, in partial fulfillment of the requirements for the degree of
Masters of Science in Water Resources Engineering and Management

Thesis Supervisor: Dr. Hamza Farooq Gabriel

NUST Institute of Civil Engineering

School of Civil and Environmental Engineering

National University of Sciences & Technology (NUST)

Islamabad, Pakistan

THESIS ACCEPTANCE CERTIFICATE

It is certified that the final copy of MS thesis written by **Mr. Muhammad Usman Ejaz**, Registration No **00000319619**, of **NUST INSTITUTE OF CIVIL ENGINEERING (NICE)** has been vetted by the undersigned, found complete in all respect as per NUST Statutes/Regulations, is free of plagiarism, errors, and mistakes and is accepted as partial fulfillment for the award of MS degree in Structural Engineering.

Signature (Supervisor), Dr. Hamza Farooq Gabriel:

H. F. Gabriel

Date:

31/08/2023

Signature (HOD):

[Signature]

Date:

31/8/23
HoD Water Resources Engineering and Management
NUST Institute of Civil Engineering
School of Civil & Environmental Engineering
National University of Sciences and Technology

Signature (Associate Dean):

[Signature] **Dr. S. Muhammad Jamil**
Associate Dean
NICE, SCEE, NUST

Date:

Signature (Dean/Principal):

[Signature]
PROF DR MUHAMMAD IRFAN
Principal & Dean
SCEE, NUST

Date:

27 SEP 2023

National University of Sciences and Technology

MASTER'S THESIS WORK

We hereby recommend that the dissertation prepared under our Supervision by:
(Student Name & Regn No.) Muhammad Usman Ejaz (00000319619).

Titled: **Application of GIS and Remote Sensing Techniques for the Estimation of Soil Erosion- Case Study: Soan River Catchment** be accepted in partial fulfillment of the requirements for the award of Master of Science degree with (B⁺ Grade).

Examination Committee Members

1. Name: Dr. Zafar Iqbal

Signature: Zafar Iqbal

2. Name: Dr. Muhammad Azmat

Signature: Muhammad Azmat

3. Name: Dr. Ammara Mubeen

Signature: Ammara Mubeen

Supervisor's name: Dr. Hamza Farooq Gabriel

Signature: H.F. Gabriel

Date: 31/08/2023

Dr. Sajjad Haider

Head of Department

Date: 31/8/23

HoD Water Resources Engineering and Management
NUST Institute of Civil Engineering
School of Civil & Environmental Engineering
National University of Sciences and Technology

COUNTERSIGNED

Date: 27 SEP 2023

Prof. Dr. Muhammad Irfan
Principal & Dean

SCEE, NUST
Principal & Dean

Author's Declaration

I Muhammad Usman Ejaz hereby state that my MS thesis titled *Application of GIS and Remote Sensing Techniques for the Estimation of Soil Erosion – Case Study: Soan River Catchment* is my own work and has not been submitted previously by me for taking any degree from this University *National University of Science and Technology* or anywhere else in the country/ world.

At any time if my statement is found to be incorrect even after I graduate, the university has the right to withdraw my MS degree.

Name of Student: Muhammad Usman Ejaz

*Muhammad
Ejaz*

Date: 31/08/2023

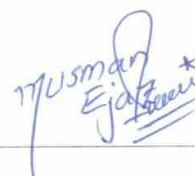
Plagiarism Undertaking

I solemnly declare that research work presented in the thesis titled “*Application of GIS and Remote Sensing Techniques for the Estimation of Soil Erosion – Case Study: Soan River Catchment*” is solely my research work with no significant contribution from any other person. Small contribution/ help wherever taken has been duly acknowledged and that complete thesis has been written by me.

I understand the zero tolerance policy of the HEC and National University of Science and Technology towards plagiarism. Therefore, I as an author of the above titled thesis declare that no portion of my thesis has been plagiarized and any material used as reference is properly referred/cited.

I undertake that if I am found guilty of any formal plagiarism in the above titled thesis even after award of MS degree, the University reserves the rights to withdraw/revoke my MS degree and that HEC and the University has the right to publish my name on the HEC/University website on which names of students are placed who submitted plagiarized thesis.

Student/Author Signature: _____

Handwritten signature of Muhammad Usman Ejaz in blue ink, written over a horizontal line. The signature includes a star symbol at the end.

Name: Muhammad Usman Ejaz

DEDICATION

Dedicated to my beloved Parents, Family and Teachers for their unwavering support throughout my academic journey.

ACKNOWLEDGEMENTS

*All praises to **ALLAH** almighty, the most Gracious and the most Merciful, Who bestowed upon me love, knowledge, passion, and strength to complete this research.*

*Nobody has been more important to me in the pursuit of this degree than the members of my family. I would like to thank my parents, whose love and guidance are with me in whatever I pursue. Without my brothers (**Waqas Ijaz, Dr. Muhammad Farhan Ejaz, Muhammad Adnan Ejaz, Noman Ejaz**) and sisters' (**Ayesha Ejaz and Aرسال Saba**) continuous encouragement, constant support, and assistance (spiritually and financially) I could not have finished this thesis.*

*I am especially indebted to my supervisor **Prof. Dr. Hamza Farooq Gabriel** for his unwavering assistance, incredible enthusiasm, valuable feedback, and astute motivation. Words cannot express my gratitude and profound admiration for him.*

*Additionally, I would like to thank my GEC members **Dr. Muhammad Azmat, Dr. Zafar Iqbal and Dr. Ammara Mubeen** for their immense help, technical know-how, and moral support.*

ABSTRACT

Soil erosion has seriously endangered the agricultural and water resource projects. As a result, the environmental issues are also increased due to the considerable amount of soil erosion at the catchment along with the agricultural land. Poor land management, deforestation, and overgrazing have reduced the natural vegetation, triggering overflow and soil loss. Soil loss data is critical for managing natural resources and boosting agricultural productivity. The majority of Pakistan is classified as having an arid climate which receives little to no rain and semi-arid climate which receives slightly higher rain than the arid climate. Before entering the Indus Basin System, nearly all hilly nullahs and hill torrents that originate from these regions' mountains receive non-perennial flows and go through substantial stretches of levelled and fertile land. These steep torrents provide flashy floods that are more intense and last for a shorter time. Flood flows travel quickly due to steep gradients, causing damage to standing crops, irrigation systems, homes, roads, and etc., as well as occasionally human life. In fact, if managed properly, these hill torrents have a great deal of potential for agriculture product to make up for the lack of food and raw materials for agro-based industries. One of Punjab Province's most significant hill torrents is the Pothowar Hill stream. Since the Pothowar area's geography is categorized as plateau and contains sporadic gulleys and deep valleys throughout, no substantial canal system can be constructed there. The provision of a local irrigation system for a solitary, tiny parcel of land with a uniform topography is mandated by the region's physical characteristics. However, unless storage systems have been made, most of the hill torrent flood flows are wasted. Punjab's Barani (rain fed) Tract (PBT), which includes the districts of Rawalpindi, Attock, Jhelum, and Chakwal, makes up around 40% of the plateau (PBT). Performing a soil erosion investigation requires a lot of effort and money. To predict soil erosion at drainage basins, several parametric models have been created. In this study, the proposed model used the methods described by Revised Morgan-Morgan-Finney model encapsulated with GIS (Geographic Information Systems) and RS (Remote Sensing). Based on the soil erosion rate in the watershed, this study also covered the effects of topography, soil erodibility, and drainage density. For rainfall intensity, LU/LC change, soil erosion, kinetic energy, and surface overflow, GIS maps

have also been created. To map and estimate the annual soil loss of the study area, analysis of the Morgan parameters has been done in ArcGIS using raster calculator from the geo-processing tools. In the watershed, the annual soil loss in 1990 was 54.04 kg/m² as there was most of the area consist of barren land, while in 2020, it is 41.09 kg/m² as the barren land is converted in to Agricultural as well as built up land.

Keywords: Soil Erosion, Remote Sensing, GIS Application, Revised Morgan-Morgan-Finney model, LU/LC, Soan River.

Table of Contents

List of Tables	xiv
List of Figures	xv
List of Acronyms.....	xvii
Chapter 1	1
1 INTRODUCTION.....	1
1.1 Background	1
1.2 Statement of Problem	3
1.3 Objectives of the Study	3
1.4 Scope of Study	4
1.5 Significance of the study	5
1.6 Organization of Research.....	5
Chapter 2	7
2 LITERATURE REVIEW	7
2.1 Soil Erosion.....	7
2.2 Soil Erosion types.....	7
2.2.1 Sheet Erosion	7
2.2.2 Gully Erosion	8
2.2.3 Rill Erosion	8
2.2.4 Tunnel Erosion.....	9
2.2.5 Channel Erosion.....	9
2.2.6 Wind Erosion	10
2.3 Past Studies on Soil Erosion	10
2.4 Role of GIS and Remote Sensing in the soil erosion estimation	13
2.4.1 Landsat-5.....	14
2.4.2 Landsat-7.....	15

2.4.3	Sentinel-2A	15
2.4.4	ALOS PALSAR.....	16
2.5	ERDAS Imagine.....	17
2.6	Image Classification.....	17
2.6.1	Supervised Classification.....	17
2.6.2	Unsupervised Classification.....	17
2.7	Accuracy Assessment.....	18
2.8	Past Studies on Land Use Land Cover Changes (LULC)	18
2.9	Research Gap.....	20
Chapter 3		21
3 METHODOLOGY		21
3.1	Study Area.....	21
3.1.1	Location	21
3.1.2	Climate.....	21
3.2	Datasets	22
3.2.1	Digital Elevation Model.....	22
3.2.2	Meteorological data	23
3.2.3	Soil Map.....	23
3.2.4	Satellite Imagery for LULC Maps	24
3.3	Hydrological Soil Group	24
3.4	Revised Morgan-Morgan-Finney Model (RMMF).....	25
3.4.1	Rainfall Energy	26
3.4.2	Runoff	27
3.4.3	Soil particle detachment by raindrop impact	28
3.4.4	Soil particle detachment by runoff.....	28
3.4.5	Transport capacity of runoff	29

3.4.6	Erosion estimation	29
3.5	Methodology	30
3.6	Description of Soil Map	30
3.7	Assessment of Historical LULC Change	31
3.8	Accuracy Assessment of Classified Images	32
3.8.1	Overall Accuracy	32
3.8.2	Producer's Accuracy	32
3.8.3	User's Accuracy	33
3.8.4	Kappa Coefficient	33
Chapter 4	34
4	Results and Discussions	34
4.1	Land Use / Land Cover Maps	34
4.2	Accuracy Assessment	34
4.3	Spatiotemporal Variation in LULC	35
4.4	Revised Morgan-Morgan-Finney Model	38
4.4.1	Rainfall Energy	38
4.4.2	Effective runoff	39
4.4.3	Soil particle detachment by raindrop impact	41
4.4.4	Soil particle detachment by runoff	43
4.4.5	Transport capacity of runoff	44
4.4.6	Erosion estimation	45
Chapter 5	48
5	Conclusions & Recommendations	48
5.1	Conclusions	48
5.2	Future Recommendations	49
References	50

List of Tables

TABLE 2.1: FEATURES OF LANDSAT-5	14
TABLE 2.2: FEATURES OF LANDSAT-7	15
TABLE 2.3: FEATURES OF SENTINEL-2A	16
TABLE 2.4: FEATURES OF ALOS PALSAR	16
TABLE 3.1: DESCRIPTION OF METEOROLOGICAL STATIONS	23
TABLE 3.2: SATELLITE IMAGERY ACQUISITION DESCRIPTION	24
TABLE 3.3: DESCRIPTION OF HSG, INFILTRATION RATE AND SOIL TEXTURE	24
TABLE 3.4: DESCRIPTION OF KAPPA COEFFICIENT RANGE AND INTERPRETATION	33
TABLE 4.1: ACCURACY ASSESSMENT OF HISTORICAL LULC'S.....	35
TABLE 4.2: LULC COVERAGE IN SOAN RIVER CATCHMENT	36
TABLE 4.3: AREA VS RANGE OF EROSION.	46

List of Figures

FIGURE 3.1: SOAN RIVER CATCHMENT (STUDY AREA).....	22
FIGURE 3.2: METHODOLOGY FLOWCHART	30
FIGURE 3.3: FAO SOIL CLASSIFICATION OF SOAN CATCHMENT & HYDROLOGICAL SOIL GROUP	31
FIGURE 4.1: LULC MAP OF SOAN RIVER CATCHMENT	37
FIGURE 4.2: LULC MAP OF SOAN RIVER CATCHMENT	38
FIGURE 4.3: ANNUAL RAINFALL MAP OF SOAN RIVER CATCHMENT (1990, 2000, 2010 AND 2020)	39
FIGURE 4.4: EFFECTIVE RAINFALL MAP OF SOAN RIVER CATCHMENT (1990, 2000, 2010 AND 2020).....	40
FIGURE 4.5: LANDUSE/LANDCOVER PARAMETERS: RAINFALL INTERCEPTION COEFFICIENT, A (%); CANOPY COVER, CC (%); CANOPY HEIGHT, PH (M), EFFECTIVE HYDROLOGICAL DEPTH OF SOIL, EHD (M); ACTUAL TO POTENTIAL EVAPOTRANSPIRATION, ET/Eo (%) AND GROUND COVER, GC (%).....	40
FIGURE 4.6: KINETIC ENERGY.....	42
FIGURE 4.7: SOIL PARAMETERS: MOISTURE CONTENT AT FIELD CAPACITY OR 1/3 BAR TENSION, MS (% WW^{-1}); BULK DENSITY OF THE TOP LAYER, BD (MGM^{-3}); DETACHABILITY INDEX, K (GJ^{-1}) AND COHESION, COH (KPA)	42
FIGURE 4.8: SOIL PARTICLE DETACHMENT BY RAINDROP IMPACT, F (KGM^{-2}).....	43
FIGURE 4.9: SOIL PARTICLE DETACHMENT BY RUNOFF, H (KGM^{-2}).....	44
FIGURE 4.10: TRANSPORT CAPACITY OF RUNOFF (KGM^{-2}).....	45

FIGURE 4.11: TOTAL ANNUAL DETACHMENT RATE OF SOIL, D (KGM^{-2})..... 46

FIGURE 4.13: AREA (KM^2) VS TOTAL ANNUAL DETACHMENT RATE OF SOIL (KG/M^2)..... 47

FIGURE 4.12: GROSS EROSION, GE ($\text{T}/\text{HA}/\text{YEAR}$) 47

List of Acronyms

ALOS	Advanced Land Observing Satellite
A	Rainfall interception by crop cover or vegetation cover
BD	Bulk density of the top soil layer (Mgm^{-3})
CC	Canopy Cover
COH	Cohesion of the surface soil
C	Crop cover Management factor
DEM	Digital Elevation Model
DSMW	Digital Soil Map of World
ET	Evapotranspiration
ESRI	Environmental Research Institute
ER	Effective Rainfall
EHD	Effective Hydrologic depth
EPM	Erosion Potential Model

ETM	Enhanced Thematic Mapper
FAO	Food and Agriculture Organization
GIS	Geographic Information System
GC	Ground Cover
GLASOD	Global Assessment of Human-induced Soil Degradation
GPCC	Global Precipitation Climatology Centre
GPCP	Global Precipitation Climatology Project
GSA	Global Sensitivity Analysis
GOES	Geostationary Environmental Satellite System
IDW	Inverse Distance Weighting
INSAT	Indian National Satellite System
KE	Kinetic Energy
KE(DT)	Kinetic Energy of Direct Throughfall
KE(LD)	Kinetic Energy of Leaf Drainage

LULC	Land use Land cover
LULCC	Land use Land cover change
Landsat	Land Remote-Sensing Satellite
LSA	Local Sensitivity Analysis
MSS	Multi Spectral Scanner
MS	Soil moisture at field capacity
MLC	Maximum Likelihood Classification
MRS	Mean Relative Sensitivity Analysis
MMF	Morgan-Morgan-Finney Model
MSI	Multi Spectral Image
MODIS	Moderate Resolution Imaging Spectroradiometer
NOAA	National Oceanic and Atmospheric Administration
NASA	National Aeronautics and Space Administration
OK	Ordinary Kriging

PH	Plant Height
PMD	Pakistan Meteorological Department
PALSAR	Polarimetric Phased Array L-band Synthetic Aperture Radar
Q	Overland flow
RUSLE	Revised Universal Soil loss equation
R	Mean Annual Rainfall
Rn	Number of rainy days
R _c	Soil moisture storage capacity
RS	Remote Sensing
RMMF	Revised Morgan-Morgan-Finney Model
SAWCRI	Soil and Water Conservation Research Institute
S ^o	Slope in Degree
SOC	Soil Organic Carbon
TC	Transport capacity

TRMM	Tropical Rainfall Measuring Mission
TMM	Thematic Mapper
USGS	United States Geological Survey
USLE	Universal Soil Loss Equation
WAPDA	Water and Power Development Authority
WMO	World Meteorological Organization

INTRODUCTON

1.1 Background

Soil erosion refers to the natural process by which the top layer of soil is gradually worn away or removed by various factors such as water, wind, or other environmental agents. It can also be caused by human activities such as deforestation, construction, or intensive farming practices, leading to the loss of fertile soil and reduced productivity of land. Soil erosion can have significant negative impacts on the environment, including water pollution, habitat destruction, and increased risk of floods and landslides. It is a serious problem, particularly in Asia, South America, and Africa, where annual rates of erosion averages around 30-40 t/ha (Gunawan et al., 2013). Due to climate change, there is acceleration in land degradation rate which is impacting the agricultural productivity as well as fertile soil in semi-arid and arid agro-ecologies. (Alam et al., 2007). In Soan catchment which lies in the Himalayan region of Pakistan, degradation rate of soil is alarming, as rainfall-runoff occurs rapidly due to the undulating features of Soan, causing soil erosion (Parveen & Kumar, 2012). Erosion reduces the productivity and fertility of the soil as it erodes the most of the topsoil (Ashiagbor et al., 2013). To investigate the process of soil loss and to assess the risks associated with the soil erosion for future planning in terms of land use, conservation of soil and management, and the modelling of soil erosion is critical (Serpa et al., 2015). Combination of field observations taken on regular basis with erosion risk modelling can assist in key decision making for efficient management of risks associated with soil erosion (Abuzar et al., 2018) (Jie et al., 2002). According to the GLASOD, due to water erosion, more than ten billion hectares surface of the earth land suffers significant soil degradation (Thompson et al., 1991). On site and off site are two types of effects of Soil erosion. On site effects are especially important for the agricultural land. Nutrients and organic matters removal reduces the fertility as well as decreases the cultivable depth of the soil resulting in the decreased production. Offsite effects are also severe as it reduces the capacity of the river, shortens the life of

the reservoirs, clogs the canals which are used for the irrigation and increases the risk of floods (Owji et al., 2012). Due to soil erosion, desertification also happens which is also alarming for the Pakistan as the climate here ranges from arid with extreme temperature variations to semi-arid. It is estimated that more than 76% of the total land area of Pakistan is affected from the soil erosion. While each year, fertile soil's erosion also occurs due to water and wind action which stands around one billion tonnes (Siddiqui et al., 2020). Natural geomorphic processes or anthropogenic activities can both cause soil erosion (Bai et al., 2008). Sheet erosion, landslides, rill erosion, inter rill, gully erosion and riverbank erosion are some of the water induced based commonly known types of soil erosion, causing the severe threat to the cultivable land and water resource management. Moreover, urban sprawl, inappropriate land use, poorly managed activities of cultivation, deforestation and overgrazing are some of the key factors which are significantly contributing to the soil erosion (Reusing et al., 2000). Effect of global warming, steep slopes, and change in basic soil properties put soil at a potential risk for erosion (Gelagay & Minale, 2016). Main reasons for uncontrolled soil erosion in Pakistan includes the poor practices of watershed management, short spell and the high intensity of the rainfall. Soil erosion in the nation's rain-fed regions is severe due to the loss of forest cover, improper land usage, growing the crops which are not suitable to the area, and overgrazing (Khan et al., 2013). The Potohar region of Pakistan has a low water retention capacity and higher water loss due to its soil texture. As a result, erosion of topsoil occurs which increases the siltation in water reservoirs such as rivers and dams. The region of Potohar has steep slopes and gets higher rainfall due to which soil erosion is most prevalent here (Hassan & Arshad, 2006). Due to pinnacle erosion, slumping and piping, a significant area of the Potohar has become steeply dissected as well as gullied (Baig et al., 2013). Food security is also impacted by soil erosion as it jeopardizes agricultural productivity (Sinha & Joshi, 2012). Serious erosion problems are caused by the removal of natural vegetation, farming without any terracing on the steep slopes and the organic matter reduction on the terraced slopes. Potohar region's agriculture is dependent on the rainfall, hence its agricultural production is lower than that of Pakistan's irrigated regions. To determine environmental effects and create plans for soil management and conservation, quantitative estimation of soil erosion at the regional level

is necessary (Alexakis et al., 2013). In recent years, Empirical, deterministic and stochastic models have been developed with varying nature of the complexity and degree of accuracy. Advancement in computational tools helped to develop such models which comply with these tools and consider the requirements of going beyond the field scale to forecast the soil loss by including sediment transport routines and to examine how soil parameters affects the erosion modelling (Panagos et al., 2014).

1.2 Statement of Problem

One of the main risks to sustainable land management is associated with soil erosion that occurs due to water. To prevent the soil erosion, effective management of the huge regions is necessary. As fertile soil is taken away by erosion from the surface of the earth and deposits in the reservoirs, such erosion poses severe issues to agriculture and to manage the water resources. Reduced usable storage space shortens the reservoir life due to sediment yield. Although soil degradation is a natural process, human activities like construction or vehicle disturbance can significantly alter its pace, as well as the movement and deposition. Water quality destruction, hazardous circumstances, and other environmental harm can all result from increased erosion and sedimentation, prompting costly maintenance. Additionally, the success of every other sector, including fisheries, industry, and livestock production, depends on the availability of water. The sole possible source that can be controlled for economic use and sociocultural advancement in the region is the flood flows of the local hill torrent. Soil conservation measures should be damaged as little as possible. Although such planning may appear challenging for vast areas, geographic information systems (GIS) can offer the means to analyze different disturbance alternatives, assess the danger of erosion, and spatially optimize conservation action.

1.3 Objectives of the Study

- To analyze the following land use parameters;
 - Soil type
 - Land cover

- Vegetation cover
- Topography
- To estimate the soil erosion by integration of Morgan approach with GIS & RS
- To estimate the sediment yield using application of soil erosion model
- To provide guidelines for soil conservation practices for the area under the study

1.4 Scope of Study

Numerous models for soil erosion have been created in recent decades. The performance of large scale field observation of erosion like continental, watershed, and national etc. is difficult, that's why models become essential estimation tools. Various empirical, stochastic, and deterministic models, possessing varying degrees of complexity and accuracy, have been developed in recent times. The development of computational tool, which consider the need to go beyond field-scale forecast of soil loss by including sediment transport routines, is aiding their progress Panagos et al. (2014). Compared to detailed process-based models, coarser empirically based models such as the Erosion Potential Model (EPM), Gavrilovic (1962), the Universal Soil Loss Equation (USLE); Wischmeier and Smith (1978), and the Revised USLE (RUSLE; (Renard, 1991)), have advantages like less requirement of data, cost of implementation is lower, easy to use, and speed of computation. The calibration and parameterization process caused errors which are the reason of poor performance Tiwari et al. (2000). Given the preceding information, the study aims to adopt a more appropriate approach by choosing the Revised Morgan-Morgan-Finney model, which is semi physically based Morgan (2001). By using semi-empirical relationships and avoiding excessive parameters and computing resources, the Revised Morgan-Morgan-Finney model maintains conceptual simplicity and operational flexibility, while also providing an in-depth understanding of soil erosion processes through the use of physical concepts. It combines the best feature of both physically based models like WEPP (Nearing et al., 1989), EUROSEM (Morgan et al., 1998) , and LISEM (De Roo et al., 1996), as well as empirical models. The Revised Morgan-Morgan-Finney model was employed to estimate soil erosion using high resolution radar DEM, Sentinel 5, 7 and 2-A land imagery, and FAO soil data. Like

physically based models, it offers a comprehensive understanding of soil erosion processes by utilizing physical concepts.

1.5 Significance of the study

Several crucial ecosystem services are provided by soil, which is an essential resource. We generate 99 percent of our food on it, along with raw materials, fibre, biofuels, and fodder (FAO 2003). Soil not only serve as a critical carbon storage and climate regulator but also holds two to three times more C than the atmosphere (Towers et al, 2006). Additionally, soils regulate water resources by dampening hydrological reactions and eliminating impurities from water that is percolating(Haygarth & Ritz, 2009). This resource and the environment are seriously threatened by accelerated soil erosion brought on by water erosion (rain splash, inter rill, gully and rill erosion, and soil piping), wind erosion, tillage erosion, and loss of soil during the harvesting of crop. In fact, several historical civilizations have fallen into disrepair because of soil erosion and deterioration brought on by unsustainable human activity.

This study will be helpful in future for the following purposes.

- Water resources management.
- Protection of Nutrients and Organic matter of Agricultural land
- In order to enhance the fertility of the soil and improve the productivity of crops
- To increase the capacity of rivers.
- Reduction in the blockage of irrigation Canals

1.6 Organization of Research

- **Chapter 1: Introduction:** Introduction of thesis topic, background, objectives and significance of the study.
- **Chapter 2: Literature Review:** A literature review of past studies on LULC, Revised Morgan-Morgan-Finney model, LULC classification and estimation of soil erosion.
- **Chapter 3: Methodology:** Methodology, the tools and techniques employed in this study, as well as the study area.

- **Chapter 4: Result and Discussion:** The results and finding are presented and discussed in this chapter including spatial distribution maps and temporal distribution graphs.
- **Chapter 5: Conclusion & Recommendation:** Overview of the findings of this study and recommendations for future studies.

LITERATURE REVIEW

2.1 Soil Erosion

Raindrop impact and running water cause soil detachment, transportation, and deposition, which collectively result in soil erosion. The land and water resources suffer severe challenges because of erosion. Erosion leads to land degradation in the form of gullies and rills as well as the loss of top fertile soil due to sheet erosion. The result is a decline in the production of the land. Sediment buildup in reservoirs, channel aggradations, and deterioration are examples of off-site issues. Agricultural production is negatively impacted by all these issues (Pimentel et al., 1995). A sluggish process that often goes unnoticed, soil erosion can sometimes happen at an alarming rate and result in significant topsoil loss. Reduced agricultural production capacity, poor surface water quality, and a broken drainage system may all be effects of soil loss on farmland.

2.2 Soil Erosion types

Types of soil erosion are discussed below.

2.2.1 Sheet Erosion

A phenomena in which overland flow or raindrop impact removes the top thin layer of the soil. It is not easy to monitor this because it is a time taking phenomena as the top layer of soil gets damaged with the passage of time. This sneaky phenomenon frequently gets unnoticed until the underlying soil is revealed. Land productivity also gets affected by the loss of the top layer as it contains a rich amount of nutrients and organic matter. Soil capacity to hold water in dry season is badly affected by erosion which has a negative impact on seeds as well as on seedlings. Such erosion damages crop and pastures, degrades the quality of water, and sediments streams, dams, lakes, and reservoirs. Sheet erosion is especially dangerous on frequently cultivated soils, barren land, or soils that have become bare due to excessive grazing of animals.

2.2.2 Gully Erosion

When small channels which are also known as rills are enlarged enough to obstruct automobile accessibility, are known as gullies or gully erosion. These larger rills have significant concentrations of high-velocity run-off water that remove a significant amount of soil. This leads to the development of severely incised gullies beside depressions and drainage lines. Scour gullies and head ward erosion are two separate types of abrupt deep and wide gullies that are produced when topsoil and subsoil are removed by swiftly moving surface water. Run-off water contained in rills or dejection removes soil particles in dredge gullies by sieving the scouring effect of flowing water on loosened particles. Commonly used materials are the size of fine to medium sand and can come from slaking, which occurs when huge wet aggregates break down. Landscapes that gently undulate are frequently associated with scour gullies. Gullies can widen due to lateral erosion, which occurs when water undercuts the sides, causing the sides to sink. Splash, sheet, and rill erosion may also occur on gully walls.

Gully erosion has some serious impacts as large amount of soil is lost. Deep broad gullies, up to 30m deep, severely limit land usage as rivers and streams water quality compromises due to silting of reservoirs and dams. Cattle and vehicle access is also effected by large gullies.

2.2.3 Rill Erosion

Rill erosion is common in farmlands of fresh cultivated lands after heavy rains, and it can also be related with sheet erosion. A surface film of water develops if rainfall is greater than infiltration. Rill erosion is triggered by the infiltration of surface water into profound and rapid channels that undergo valleys or low regions through farmlands. These channels are the ideal means for transporting sediment because the shearing action of the water can split, gather, and dislodge the particles of soil. The transitional phase between sheet and gully erosion is frequently used to define rill erosion. The surviving subsoils are frequently far less productive because of the loss of topsoil and nutrients, which significantly lowers productivity. Off-site soil deposition is also related to siltation of streams, dams, and reservoirs, which impairs the quality of water and harms aquatic

habitats. After tillage, rill erosion is frequently observed in crop regions because it occurs frequently on agricultural land without vegetation. Cultivated topsoil that are atop denser, more solid subsoils frequently experience rill erosion after heavy rain. Texture-contrast (duplex) soils and poorly managed pastures with overgrazing are both vulnerable.

2.2.4 Tunnel Erosion

Water can create subterranean pathways by eroding or infiltrating through responsive subsoil. Tunneling is usually linked to poor natural vegetation, sheet type erosion, and higher surface flow. Water seeping into and through dispersive subsoils causes tunnel erosion. It frequently happens because of water building up and migrating down fractures or channels, into rabbit burrows, or into cavities created by old tree roots. Tunnels need a suitable slope to begin the drainage velocity needed to force groundwater through the earth. As the tunnel gets longer, the ceiling collapses in places, creating potholes and gullies. Such erosion results in decreased capacity for production, the deposit of barren substrata in more productive areas, and heavy sedimentation in rivers or streams. In extreme scenario, tunnels can be dangerous because they can collapse, obstruct safe passage, and create gullies. It typically occurs on cleared hill slopes with 300–650 mm of annual rainfall, especially on erodible soil.

2.2.5 Channel Erosion

In drainages and waterways, both embankment and bed erosion occur. The sudden loss of embankment and bed caused by the flow of water is known as the channel erosion. It typically happens when the stream flow is high. It is frequently mistaken for gully erosion because it's so similar to intermittent streams. The lateral (side) degradation and collapsing of watercourse or waterways usually result in high sediment loads in waterways. The problem often begins when catchments with sparse vegetation cover experience heavy rains that result in excessive run-off. The downstream of a catchments will receive most of the high volume and velocity runoff that results. Erosion of the stream bank and stream bed happens when the stress put on the soil by these stream flows is greater than the soil's capacity to withstand them. When the amount of sediment increases, the streams which are moving fast grind and dig their sides into the

surrounding terrain. Sediment is eventually dumped further downstream or eventually in reservoirs and dams as a result of the stream becoming overloaded or its flow rate being lowered. The loss of fertile land caused by bank and bed erosion is not the only consequence of significant changes in the channel of a river or creek; such changes also frequently obstruct access to properties. Lateral soil deposition results in sedimentation in reservoirs and issues on fertile land downstream.

2.2.6 Wind Erosion

The transportation and deposition of the particles of soil by air is known as wind erosion. The erosion by wind is obvious. Water erosion is a concern, but it is typically far more severe. It happens due to the exposure of soil cleared of vegetation to strong winds. Soil particles are carried away by wind in suspension when the velocity of the wind exceeds the gravitational and cohesive forces acting on them. As part of this process, the soil particles are separated, and the coarser and less fertile material is left behind, whereas the finer material, consisting of organic matter, silt, and clay, is carried away by suspension. Farming areas located inland, especially those involved in crop cultivation, are highly vulnerable to wind erosion if they have annual rainfall less than 375 mm and are characterized by sandy soils containing low levels of organic matter

2.3 Past Studies on Soil Erosion

According to published research, scientists are almost unanimous in their belief that soil resources on Earth are in jeopardy due to global erosion (Wilkinson & McElroy, 2007); (Van Oost et al., 2007) ; (Montgomery, 2007). Soil erosion is a significant global problem, resulting in the annual loss of 430 million hectares of agricultural land and the erosion of approximately 75 billion metric tons of soil each year, according to (Pimentel et al., 1995). (Lal, 1990). Regions of the world that are considered erosion hotspots include the Highlands of Central America, South Asia's Himalayan region, Africa's sub-humid and semi-arid areas, the Andean region of the Caribbean, and the Loess Plateau of China (Cerdà et al., 2021). Mitigation of climate change, soil erosion protection and the fertility of soil are types of environmental benefits obtained from forests. (Denboba, 2005); (Aticho, 2013). On the other hand, the expansion of agricultural land by cutting

down forests is the result of the growth of human population (Kassa et al., 2017). Forest land is often changed to agricultural land in order to boost agricultural productivity, which is not an issue if the shift in land use is maintained sustainably. Deforestation on steep terrain and weak soils results in severe soil erosion, which damages the soil severely. Extreme soil deterioration, agricultural land usage unsustainability and rising conversion rates of forests, all contribute to the poverty-environment trap (Sonneveld & Keyzer, 2003). Soil erosion diminishes the agricultural value of fields by causing physical, chemical, and biological degradation. The primary cause of the deterioration in soil fertility is runoff loss of nutrients of soil (Sahu et al., 2015); (Kurothe et al., 2014). The economies of the damaged regions are negatively impacted by soil erosion, which results in severe environmental and economic resource losses (Boardman et al., 2019); (Baliani & Vaezi, 2017). The type of agricultural systems and accessible soil management techniques influence the number of nutrients transferred. Crop land stability is affected by agro-environmental factors, including water-induced runoff and soil erosion (Kocyigit & Demirci, 2012). Such agro-environmental factors are based on topography and soil characteristics, but these factors can alter because of the usage of land and climate (Bai et al., 2012). The impact of forest extraction on soil nitrogen losses and the environment is of significant importance and cannot be emphasized enough. Using more and more limited forest resources to cover the rising demand for fuel results in environmental damage and soil nutrient loss (Gabriel & Ayuba, 2006). Deforestation is the process of removing vegetation from a forest due to human or natural activity. Clearing fields of trees can lead to severe erosion, nutrient depletion, forest degradation, and flooding, particularly during heavy rainfall, as there are no trees or roots to provide soil protection (Sayyad et al., 2019). The depth of the topsoil, structure, texture, and nutrients, as well as the amount of bulk density and organic matter, which are all factors in crop yield and soil fertility, are all impacted by erosion (Lal, 1988). Soil erosion results in the loss of essential nutrients, including potassium (K), nitrogen (N), and phosphorus (P), as well as other vital components such as soil micro fauna, microbial biomass, some trace elements, and water retention capacity, and organic carbon content. (Berhe et al., 2007). Erosion is a complicated issue, and it can only be controlled to the proportion that the effect of the variables speeding up the erosion can be reduced. Adopting the

necessary measures to combat soil erosion is essential. Compared to soils with no erosion, increasing the use of inorganic fertilizers may not increase crop productivity (Shah & Wu, 2019). As the importance of carbon sequestration to mitigate climate change becomes more widely acknowledged, the significance of organic carbon in soil is gaining momentum. If a land has little vegetation, it may be susceptible to erosion (Vishnudas, 2006). The primary purpose of vegetation cover is to prevent erosion (He et al., 2007). Rainfall is intercepted by vegetation, which enhances water infiltration and dissipates the energy of moving water (Blanco & Lal, 2008); (Livesley et al., 2014). The soil environment is the primary determinant of the availability of micronutrients. The lack or presence of micronutrients and macronutrients affects the soil's fertility. Numerous research studies have shown that elements including soil pH, texture, and organic matter have an impact on the number of micronutrients (Nazif et al., 2006). The formation of sediment aggregates affects the movement and deposition of soil organic carbon on slopes. This further restricts the downward transmission of SOC in the relevant watershed. Due to precipitation, a significant portion of the displaced soil organic carbon remains within the watershed; this shows that organic carbon has accumulated at the watershed's edges and that most of it has mineralized just before reaching the river systems (Lal, 2005). The LULC change brought about by human-induced land use practices is a significant global change in climate (Hansen et al., 2013);(Turner et al., 2007). In general, different land use methods exist over the world, but they always lead to the same thing: meeting of urgent human demands, frequently at the expense of degradation of environmental quality (Kalnay & Cai, 2003); (Lambin & Meyfroidt, 2011); (Daily et al., 1997). Technical expertise on the ecological impact of changes in land use is essential to effectively balance human needs with the preservation of other ecosystem functions. This is because it enables us to manage the possible trade-offs that may arise between the two (Bagley et al., 2012). The type of LULC modification and the ecosystem circumstances affect these reactions. Soil is a critical resource in land use because it contributes to a landscape's five main functions, including water retention, nutrients cycling, physical stability, buffering, biodiversity, and ecosystems (Braumoh & Osaki, 2010); (Koch et al., 2013). Mitigation of climate change and the services of ecosystem affects the soil condition (Bringezu et al., 2014). Much research (De Groot et

al., 2002) describe the ecosystem services, but soil is not fully taken into account in these studies. Increased understanding of the various ways soils sustain environmental quality has led to a global push for evaluation and monitoring of this essential resource (Doran & Parkin, 1994). Due to their substantial influence on a nation's economic status, soils should be incorporated into the ecosystem services frameworks. It is necessary for effective environmental policy. Globally, soils are deteriorating as a result of processes such as salinization, erosive compaction, erosion, anaerobiosis, nutritional imbalance, and organic matter depletion (Lal, 2001). The average annual soil loss in Europe caused by rill and sheet erosion is $2.46 \text{ Mg ha}^{-1}\text{yr}^{-1}$. (Panagos et al., 2015). According to (Lamb et al., 2005), About one-third of the world's land has been negatively impacted by soil erosion on a global scale. , whereas in the tropics accelerated soil erosion has affected up to 500 million hectares (Solaimani et al., 2009). In the twenty-first century (Lal, 2001), it is anticipated that soil resource erosion will continue to be accelerated, especially in emerging nations. The majority of the carbon-related exchanges between the earth's surface and atmosphere are caused by changes in land cover and land use, even though other factors may also play a role. (Change, 2013). Furthermore, it has been established that alterations in land use are the second most significant source of greenhouse gases in the atmosphere, comprising 12-20% of the overall carbon footprint. (IPCC, 2007). Soil erosion is the most significant kind of land degradation caused by LULC change, which is second to none (Lal, 2001). Globally, soil loss from earth's surface due to erosion has an impact on the yield of natural systems, including agricultural land, range lands, and forest lands (Pimentel & Burgess, 2013). Water erosion has negatively impacted 1064 million hectares of land worldwide, with 751 million hectares experiencing severe damage. (Lal, 2001).

2.4 Role of GIS and Remote Sensing in the soil erosion estimation

Remote sensing methods have been widely used to study erosion processes since the 1990s. In this stage of development, the focus of Earth observation has shifted from single-field surveys to meeting the needs of the overall development of modern society. Due to the range of sensors on satellites orbiting the Earth, remote sensing is a crucial tool in estimating erosion at different geographical scales. . According to studies, using

remote sensing techniques can help locate degraded sites and keep track of regional erosion processes. (Sepuru & Dube, 2018); (Tarariko et al., 2019). Sentinel, Landsat, and MODIS satellites are used to collect geographical data on the area, including elevation, LULC, soil moisture, snow cover, and evapotranspiration. While NOAA, TRMM, GOES, and INSAT are utilized to gather data on the region's climatology (Abijith et al., 2020). A huge quantity of geographic data can be saved, retrieved, and managed using a geographic information system (GIS), which enables complex real-time problems to be solved. After analyzing the necessary GIS data, predetermined output layers are produced for a variety of uses. Cross sections, LULC, and other attributes could all be visualized in different dimensions. It is therefore clear that GIS has the ability to merge human and computer input to produce relevant geographic information (Tariq et al., 2020).

2.4.1 Landsat-5

On March 1, 1984, NASA launched Landsat 5, a low orbit satellite that contained the Multispectral Scanner (MSS) and Thematic Mapper (TM) instruments. The satellite produced imagery of the Earth for over 29 years, making it the longest-serving satellite in history, until it was decommissioned on June 5, 2013. Features of Landsat 5 are given in Table 2.1.

Table 2.1: Features of Landsat-5

Parameters	Landsat-5
Launch Date of Mission	01-03-1984
End Date of Mission	05-06-2013 The MSS instrument stopped acquiring data in 1999, while the TM instrument ceased operations in November 2011. The MSS was reactivated in 2012, albeit with limited acquisitions until January 2013.
Orbit Height of Mission	705 km
Orbit type of Mission	sun-synchronous near-polar orbit
Orbit Period	99 minutes
Repeat Cycle	14 days

Inclination	98.2 degree
--------------------	-------------

2.4.2 Landsat-7

ETM+, an enhanced thematic mapper, supports the Landsat 7 satellite. Thematic Mapper (TM) was equipped with various essential features, including a 15-meter spatial resolution panchromatic band, an integrated full-aperture solar calibrator, 5% absolute radiometric calibration, and a thermal infrared channel with four times the spatial resolution of its predecessor. Since June 2003, the sensor has been acquiring and transmitting data with gaps due to the malfunction of its Scan Line Corrector (SLC) (USGS.gov | Science for a Changing World n.d.). Landsat-7 features are given in Table 2.2.

Table 2.2: Features of Landsat-7

Parameters	Landsat-7
Launch Date of Mission	15-4-1999
End Date of Mission	Still operating
Orbit Height of Mission	705 km
Orbit type of Mission	sun-synchronous polar
Orbit Period	99 minutes
Repeat Cycle	Average 16 days
Inclination	98.2 degree
Crossing time of Equator	10:00 – 10:15 am
On-board sensors provided under TPM	(ETM ⁺)

2.4.3 Sentinel-2A

Sentinel-2, an Earth observation project, combines Sentinel-2A and Sentinel-2B, two spacecraft with similar multispectral instruments (MSI). It collects data in thirteen separate bands with varying spatial resolutions of 10m, 20m, and 60m. According to the orbit's design, a return visit to the equator takes five days. This satellite orbits the planet at a height of around 786 kilometers. The 290km swatch width of the Sentinel 2 mission was reported by (USGS.gov | Science for a Changing World in n.d.). Features of Sentinel-2A are given in Table 2.3.

Table 2.3: Features of Sentinel-2A

Parameters	Sentinel-2A
Launch Date of Mission	23-05-2015
End Date of Mission	Still operating
Orbit Height of Mission	786 km
Orbit type of Mission	sun-synchronous orbit
Orbit Period	100.6 minutes
Repeat Cycle	5 days
Inclination	98.62 degree
Crossing time of Equator	10:30 am
On-board sensors provided under TPM	Multispectral Instrument (MSI). Covers 13 spectral bands (443–2190 nm). Swath width of 290 km. Spatial resolution of 10 m (four visible and near-infrared)

2.4.4 ALOS PALSAR

Between 2006 and 2011, PALSAR's L-band synthetic aperture radar (SAR) conducted comprehensive day and night observations under all weather conditions, including repeat-pass interferometry. Data from PALSAR is obtained from multiple observation modes, each with different resolution, off-nadir angles, swath width, and polarization. PALSAR was one of the three sensors built for the Advanced Land Observing Satellite-1 (ALOS), or DAICHI, which was intended to assist in precise regional land-cover observation, catastrophe monitoring, and resource surveys. ([ALOS PALSAR – ASF n.d.](#)). Features of ALOS PALSAR is given in Table 2.4.

Table 2.4: Features of ALOS PALSAR

Parameters	ALOS PALSAR 1	ALOS PALSAR 2
Launch Date of Mission	24-01-2006	24-05-2014
End Date of Mission	22-04-2011	In operation
Orbit Height of Mission	691.65 km (ALOS 1)	628 km
Orbit type of Mission	Sun synchronous, Sub	Sun synchronous, Sub

	recurrent.	recurrent.
Orbital Period	98.7 minutes	
Repeat Cycle	46 days	14 days
Inclination	98.16 degree	97.19 degree

2.5 ERDAS Imagine

In a single, potent, and handy package, the ERDAS IMAGINE system combines spatial image processing and analysis, remote sensing, and GIS functionality. ERDAS IMAGINE makes it simple to produce high-value flythrough videos and cartographically improved deliverables, including 2D and 3D images and 3D quality map compositions. ([ERDAS IMAGINE 2020 Release Guide | Safety, Infrastructure & Geospatial Division, n.d.](#)).

2.6 Image Classification

The act of categorizing pixels into a predetermined number of data categories or classes based on the data values contained within the pixels is referred to as image classification or segmentation. A pixel is allocated to a class if it achieves a specific set of criteria.

2.6.1 Supervised Classification

The user has significant control over supervised classification. The user selects pixels that approximate LULC characteristics that they can identify using maps, aerial photographs, or ground truth data during this process. The user must be familiar with the study region, the dataset obtained from satellite, and the desired number of classes before doing supervised classification. By recognizing patterns, the user can instruct the machine to find pixels with comparable characteristics. If the image is accurately categorized, the classes that are produced match the categories found in the data.

2.6.2 Unsupervised Classification

Compared to supervised classification, unsupervised classification uses greater computer assistance. It enables the definition of certain parameters the computer will use when

searching for statistical patterns in the data. These patterns might or might not be related to important study area characteristics, including easily recognizable LULC patches. They are simply a collection of pixels having similar spectral characteristics. The data itself serves as the basis for this categorization. When there is little available prior to categorization regarding the data, this strategy is often used. Then, it is the user's responsibility to give the ensuing classes a purpose.

2.7 Accuracy Assessment

To determine the precision and completeness of the classification phase, classed data is compared with geographical data that is assumed to be accurate. The ground truth data are typically used to obtain the presumptive data. In essence, classification accuracy is understood to represent how closely the categorized image resembles reality or adheres to the truth. Anomalies are frequently present in LULC categorized maps obtained from satellite data for a variety of reasons, including satellite image collection techniques and classification algorithms. Evaluation of classification output is crucial during the classification process as a result. In this paradigm, categorized maps derived from satellite data are analyzed using a confusion matrix.

A confusion matrix illustrates the number of observations assigned to each class compared to their actual class. The columns display ground truth information, and the rows display a LULC map produced from remotely sensed data. The reference data and the training data that were used for classification should be kept apart; it should be mentioned. To assess the correctness of the categorized maps, statistical measures such as commission errors, omission errors, overall accuracy, and a kappa coefficient are produced by the matrix's columns and rows (Green et al., 2017).

2.8 Past Studies on Land Use Land Cover Changes (LULC)

Many people consider LULCC to be one of the principal contributors to global environmental change, owing to its wide-ranging impacts. In the Anthropocene epoch, LULCC are inextricably linked to the growth of commercial activity, mechanized agriculture, unchecked infrastructure sprawl, and a broad demographic transition from

rural to urban areas. Alterations in LULC, primarily caused by human biomes, such as modifications in vegetation types, LULC practices, and spatial patterns, are anticipated to have a substantial influence on the hydrological characteristics of basins. These changes may alter the watershed's hydrology by modifying LULC canopy interception, soil properties, infiltration, albedo, and evapotranspiration. As a result, the interplay among these variables at the basin level can be complex and may lead to variations in the timing and magnitude of hydrological processes across space and time (Ellis et al., 2020); (Kiprotich et al., 2021). Land usage encompasses a wide range of concepts and meanings. According to (Lambin & Meyfroidt, 2011), Land cover includes a range of features found on the earth's surface and subsurface, such as the type of soil, living organisms, topographic features, man-made structures, and water resources above and below the ground. Land is subjected to pressures caused by poor management practices, resulting in land degradation, reduced crop yields, soil erosion, deforestation, pasture destruction, and the depletion of water resources to meet the growing demand of the population. (Nabhan, 1999). (Bagley et al., 2014) added that the conversion of natural entities to production activities through changes in land use and cover has resulted in a threat to environmental functioning. Earlier studies have established a robust association between alterations in land use and land cover (LULC) and environmental modifications on a global scale, such as greenhouse gas emissions, biodiversity decline, climate change, and soil resource depletion (Wang & Yang, 2012). Land use and land cover change (LULCC) is the result of complex interactions between human activities and the natural environment, and it refers to the transformation of different land use types (Bruijnzeel, 2004). LULCC is a substantial contributor to planetary change and has a big impact on biodiversity, biological cycles, and ecosystem processes (Halmy et al., 2015), (Akinyemi, 2021), (Foley et al., 2005). Additionally, LULCC and the social economy's sustainable growth are closely related (Hansen et al., 2013), (Searchinger et al., 2018). Large portions of the earth's surface have experienced LULCC (Gerssen-Gondelach et al., 2017), (Llerena-Montoya et al., 2021). When there is a rapid economic development, land use changes at a faster pace, and the distinction between different land use types becomes more pronounced (Mena et al., 2011).

2.9 Research Gap

An essential component of the nature, soil is crucial for the agriculture, ecosystems, water channels, and dam's capacity. There are different method for erosion estimation and RUSLE model is widely used. However, RUSLE can estimate erosion in plain fields with greater accuracy because it was designed for plain fields. Although it is also used in the erosion estimation of hilly areas but the model used for hilly as well as plain areas is Morgan-Morgan-Finney model. In this study Revised Morgan-Morgan-Finney model has been used to estimate soil erosion as our area "Soan River catchment" consists of hilly areas and plain fields. This is the first study in recent times which is carried out by that model and this study will help to improve land use and land cover changes of region and will help to enhance the life and capacity of water bodies. Furthermore, it will be helpful in policy making regarding water resources management for agriculture and domestic purposes.

METHODOLOGY

3.1 Study Area

3.1.1 Location

Located in the sub-Himalayan region of Pakistan, the Soan River basin covers an area of 6542 km² and features elevations ranging from 219 to 2226 m. Approximately 60% of the area is characterized by a flat to gentle slope, measuring between 0 to 5 degrees, while 29% of the region features a medium slope ranging from 5 to 15 degrees. Steep slopes, measuring between 15 to 30 degrees, cover roughly 9% of the land, while very steep slopes exceeding 30 degrees cover approximately 2% of the area. Most of the soils in the area have sufficient drainage, are deep and diverse, and exhibit moderate levels of calcareousness. They vary in composition from clay loam to silty clay loam. Numerous gravel and rock outcrops are visible on the study area's western side, in close proximity to the Rawal lake drain. Although the Miocene Murree Formation rocks are visible in certain areas, most of the land is covered by alluvium. Agriculture in the region relies on a combination of rain, springs, wells, and small/mini dams that maintain perennial poultry. Plains, steep terrain, and terraced slopes along riverbanks make up the majority of the farmed area. The primary crops cultivated in rain-fed conditions include wheat, chickpeas, groundnuts, millets, sorghum, oilseeds, and fodder. Vegetables and orchards containing guava, citrus, loquat, and pears are grown in areas with access to irrigation water from dams, dug wells/tube wells, and springs.

3.1.2 Climate

The weather in the region is of a continental and subtropical nature, characterized by hot summers and mild winters. The yearly precipitation varies from approximately 450 to 1750 mm (Ullah et al., 2018),(Cheema & Bastiaanssen, 2012). Nearly two-thirds of the total precipitation, which falls between July and September, is attributed to the monsoon

season. The temperature in winter is 4°C to 25°C and summer temperature ranges 15°C to 40°C (Ur Rahman et al., 2020). The study area map is presented in Figure 3.1.

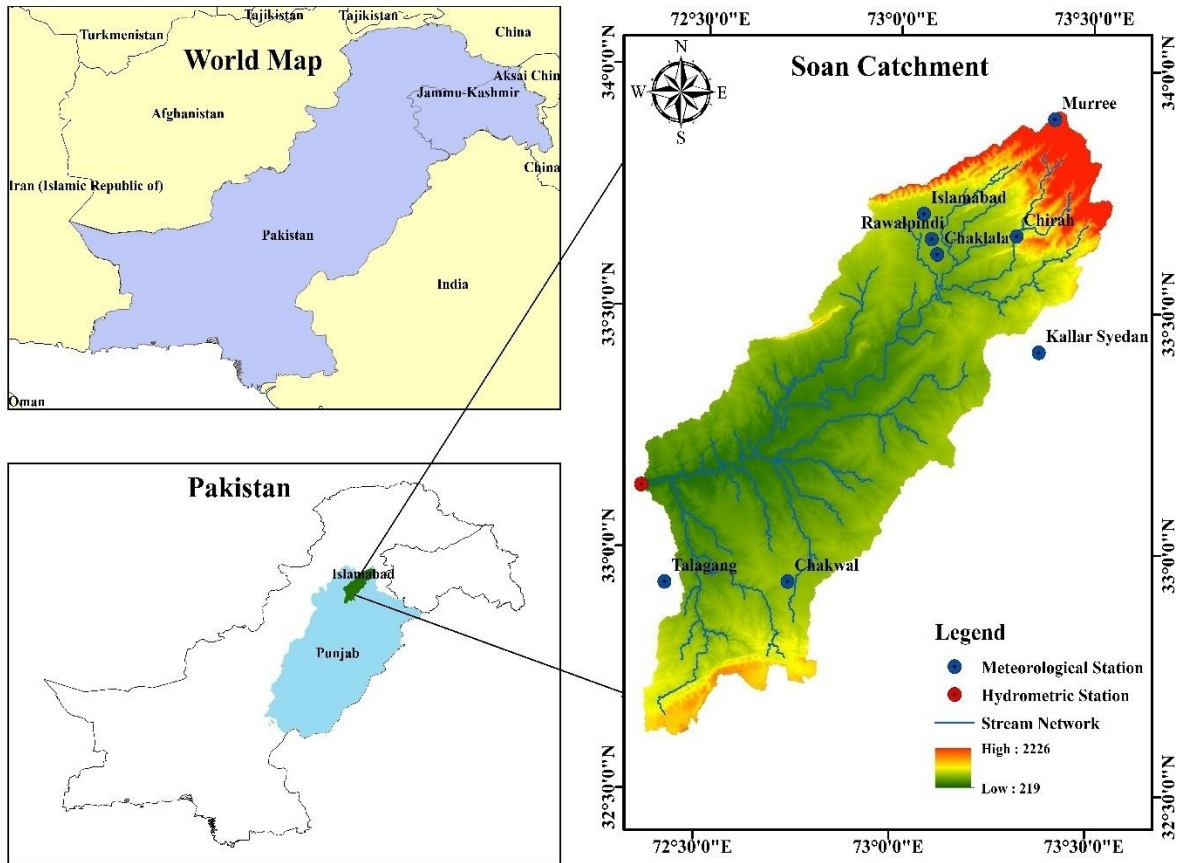


Figure 3.1: Soan River Catchment (study area)

3.2 Datasets

Geospatial datasets, such as soil maps, digital elevation models (DEM), LULC maps as well as precipitation data are necessary for the estimation of soil erosion.

3.2.1 Digital Elevation Model

A digital elevation model (DEM) is a cartographic dataset that depicts a continuous surface of topographic elevations through a series of cells. A digital elevation model (DEM) of ALOS PALSAR with a spatial resolution of 12.5 meters was made available by the UAF Alaska Satellite Facility (<https://vertex.daac.asf.alaska.edu/#>). The obtained DEM was used to obtain information about the catchment terrain, which was then used to

define stream networks, delineate watersheds, slope of catchment, and determine elevation.

3.2.2 Meteorological data

The observed climatic data was supplied by the Pakistan Meteorological Department (PMD), the Surface Water Hydrology Project- WAPDA (SWHP-WAPDA), and the Soil and Water Conservation Research Institute (SAWCRI) in Chakwal. The observed station details are presented in Table 3.1.

Table 3.1: Description of Meteorological Stations

Sr.No	Station	Longitude	Latitude	Altitude (a.m.s.l)	Data range (Precipitation)	Source
1	Chaklala	73° 5 ' 60"	33° 37 ' 0"	500	1980-2020	PMD
2	Chakwal	72° 43 ' 48"	32° 55 ' 59"	521	1990-2020	PMD
3	Chirah	73° 18 ' 18"	33° 39 ' 24"	579	1986-2020	WAPDA
4	Islamabad	73° 5 ' 60"	33° 37 ' 1"	508	1960-2020	PMD
5	Kallar Sayyedana	73° 22 ' 0"	33° 25 ' 0"	518	1987-2020	SWHP
6	Murree	73° 24 ' 0"	33° 53 ' 60"	2168	1980-2020	PMD
7	Rawalpindi	73° 5 ' 6"	33° 38 ' 53"	540	1981-2020	PMD
8	Talagang	72° 24 ' 50"	32° 55 ' 37"	457	1989-2020	SAWCRI

3.2.3 Soil Map

Soil datasets are crucial components in erosion models for defining various layers and types of soil properties, including bulk density, soil depth, hydraulic conductivity, particle-size distribution, texture, pH, organic carbon content, and hydrologic soil groups. The open-source FAO-Digital Soil Map of the World (DSMW), which has a spatial resolution of 30 arc-seconds and a scale of 1:500,000, is created and maintained by the United Nations Food and Agriculture Organization (FAO). ([FAO/UNESCO Soil Map of the World | FAO SOILS PORTAL | Food and Agriculture Organization of the United Nations n.d.](#)).

3.2.4 Satellite Imagery for LULC Maps

The USGS Earth Explorer (<https://earthexplorer.usgs.gov/>) was used to obtain remote sensing satellite data. For evaluating the spatio-temporal trends of LULC, satellite imagery from 1990, 2000, 2010, and 2020 were collected using Landsat 5 TM, Landsat 7 ETM+, and Sentinel-2A sensors which has a spatial resolutions of 30 m, 30 m, and 10 m, respectively. The imagery was acquired with the idea that there should be minimal cloud cover (Table 3.2).

Table 3.2: Satellite Imagery Acquisition Description

Sr. No.	LULC Year	Source	Resolution	Date of Acquisition	Cloud Cover
1	1990	Landsat-5	30 m	24-05-1990	1%
2	2000	Landsat-7	30 m	13-06-2000	1%
3	2010	Landsat-7	30 m	18-06-2010	2%
4	2020	Sentinel-2A	10 m	29-06-2020	0%

3.3 Hydrological Soil Group

The Hydrologic Soil Group (HSG) varies according to the type of soil and describes its infiltration capacity and the speed of **movement of** water through it. The four different categories of HSGs are listed in Table 3.3, along with brief descriptions of each. When calculating an HSG for a soil, the bare soil surface is considered. ([Hydrologic Soil Groups - Overview n.d.](#)).

Table 3.3: Description of HSG, infiltration rate and soil texture

Soil Group	Description	Infiltration Rate (mm/hour)	Soil Texture
A	Soils have high rates of infiltration and poor runoff potential. Consists of deep sands with little clay or silt, as well as deep, highly permeable loess.	Infiltration rate is high and has a range b/w 8 to 12	Sandy Loamy, Loamy Sand and Sand.

B	Moderate runoff potential and infiltration rate. Mostly sandy soils that are shallower than A and loess that is shallower or less aggregated than A, but the group as a whole exhibits above-average infiltration following thorough wetting.	Infiltration rate is 4 to 8	Loam and Silt loam.
C	Lower infiltration rate and higher runoff Potential. Contains shallow soils and soils with a less amount of clay and colloids than those in group D. The group's penetration is below average.	Infiltration rate is 1 to 4	Sandy Loam and Loam
D	Very low infiltration rate and highest potential of runoff. The group consists primarily of clays with a high swelling percentage, but it also contains some superficial soils with nearly impervious sub horizons near the surface.	Very low infiltration rate 0 to 1	Clay loam, silty clay loam, sandy clay and clay

3.4 Revised Morgan-Morgan-Finney Model (RMMF)

It is a semi-physically based model and divides the erosion process in two phases, one is water phase and other is sediment phase. Fundamental elements of water phase are height and intensity of precipitation on annual basis. These components are utilized to compute the overland flow that contributes for the transportation of soil particles and precipitation energy which is required to dislodge soil particle due to raindrop impact.

In sediment phase, we used aforementioned variables as input, which is made up of two parts: runoff transport and splash detachment. Splash transit is not taken into account. The annual rate of soil loss is determined by comparing the expected splash detachment rate of rain with the transport capacity of overland flow, and selecting the lower of the two numbers (Morgan, 2001). Morgan developed the model (Morgan et al., 1984) predictive to solve the flaws and constraints in its original form (MMF; Morgan-Morgan-Finney). These constraints encompass challenges with measurement of effective hydrologic depth, accessibility, and estimation (detachment of soil particle due to the

impact of rainfall: changed description, taking into account the leaf drainage which is dependent on the height of the fall); (Wischmeier & Smith, 1958) of specific parameters. Moreover, a factor for the detachment of soil particle by surface runoff/overland flow was included, especially in locations with steep topography and where runoff is routed into rills.

3.4.1 Rainfall Energy

Taking into account how precipitation is divided when it reaches plant canopy, the method used to calculate rainfall energy considers the protective covering provided by canopy which reduces the volume and kinetic energy of the rain that reaches the soil surface through leaf drainage and direct throughfall especially in terms of cover, height, and ground cover density. Before available to plants, precipitation that is added and held in the soil is known as effective rainfall.

$$ER = RA \quad 3.1$$

Where R (mm) denotes the mean annual precipitation and coefficient of rainfall interception is denoted by “A” (%). The ER is divided into two parts: direct through fall (DT), which flows freely to the surface of soil, and interception by plants and flows toward surface is leaf drainage (LD). Canopy cover in percentage (CC), stated as a ratio between 0 and 1, and determines the division.

$$LD = ER \times CC \quad 3.2$$

$$DT = ER - LD \quad 3.3$$

The calculation of direct through-fall kinetic energy (KE (DT), J m⁻²) is based on the rainfall intensity (I, mm h⁻¹). Empirical equations have been developed for different climatic conditions worldwide to establish the correlation between the intensity of precipitation and its kinetic energy (KE, J m⁻² mm⁻¹). (Hudson, 1965), (Zanchi & Torri, 1980), (Rosewell, 1986). If there are no field observations available, a standard value of I is used for each climatic region, Such as for temperate climate is 10, for tropical climate is 25, and for climate which has intense seasonal fluctuation is 30.

$$KE = 11.9 + 8.7 \log_{10} I \quad 3.4$$

$$KE (DT) = DT (11.9 + 8.7 \log_{10} I) \quad 3.5$$

Leaf drainage kinetic energy is determined by using the plant canopy height (Breshears et al., 2003).

$$KE (LD) = (15.8 \times PH^{0.5}) - 5.87 \quad 3.6$$

PH (m) denotes the altitude at which raindrops begin their descent from the crop or vegetation cover and eventually reach the ground. If Equation (3.6) yields a negative value, then the KE (LD) parameter is assigned a value of zero.

Effective rainfall's total energy can be calculated as following

$$KE = KE (DT) + KE (LD) \quad 3.7$$

3.4.2 Runoff

The methodology used for estimating runoff is (Kirkby, 1976), (Hassan, 1979). It assumes that when daily precipitation surpasses the moisture storage capacity of soil. Additionally, it assumes that the daily precipitation can be characterized by exponential frequency distribution (Morgan et al., 1984).

$$Q = R \times \exp(-R_c / R_o) \quad 3.8$$

$$R_o = R / R_n \quad 3.9$$

$$R_c = 1000 \times MS \times BD \times EHD \times E_t / E_o \quad 3.10$$

Yearly runoff is denoted by Q, which is estimated by using a methodology based on several factors, mean annual rainfall is denoted by R, soil moisture storage capacity is denoted by R_c, average amount of rain per erosive rain day is denoted by R_o, and number of rainy days per year is denoted by R_n. Soil's top layer bulk density is represented by BD (Mg m³), soil's moisture content at field capacity is represented by MS (% w w⁻¹), soil's effective hydrologic depth is represented by EHD (m) (It is the depth where generation of

runoff is controlled by storage capacity of moisture, surface crust absence or presence of, and the presence of layer which is impermeable), and R_o (mm) the mean rainfall per erosive rain day.

3.4.3 Soil particle detachment by raindrop impact

The estimation of soil particle detachment caused by raindrop impact can be done by following equation

$$F = K \times KE \times 10^3 \quad 3.11$$

Where KE is the total energy of the effective ($J m^{-2}$) and K ($g j^{-1}$) is the soil detachability index, which measures the erodibility of the soil. It is the weight of soil that is separated from the soil mass per unit of rainfall energy. The dependency of variation of index is on internal and external factors. Internal factors are of two types, one is mechanical factor and other is chemical factor. First type includes the texture of soil, stability of aggregate, infiltration capacity and shear strength while second type includes capacity of cat ion exchange, carbon to nitrogen ratio, pH, and content of organic matter. External factors includes morphology, vegetation cover, rainfall, geology and man-made disturbance (over grazing, tillage, cultivation, deforestation, etc.). Small cohesive particles are detachment resistant as compared to Large, heavy one and they are easier to transport.

3.4.4 Soil particle detachment by runoff

(Quansah, 1982) states that, the estimation of soil particle detachment caused by runoff is determined by considering several factors. These factors includes the amount of runoff, the ground cover percentage, steepness of slope ($S, ^\circ$) and soil resistance to erosion, which is measured by it's cohesion . For non-cohesive, loose soil, the value of Z is 1. When ground cover is not protecting the soil, then particles of soil detached by runoff.

$$Z = 1 / (0.5 \times COH) \quad 3.12$$

$$H = Z \times Q^{1.5} \times \sin S \times (1-GC) \times 10^3 \quad 3.13$$

3.4.5 Transport capacity of runoff

The transportation potential of runoff can be estimated by the following equation

$$TC = C \times Q^2 \times \sin S \times 10^3 \quad 3.14$$

There are two factors of USLE, one is C and the other one is P. Combination of both these factors gives us the value of C which will be used in above equation while S (°) is slope steepness.

3.4.6 Erosion estimation

To estimate the annual erosion rate of soil, the detachment of soil particle caused by runoff and raindrop impact are added together.

$$D = F + H \quad 3.15$$

By comparing the rate of detachment to the annual transport capacity of runoff, the lesser of the two values is determined to be the annual rate of erosion (GE).

3.5 Methodology

The methodology flowchart is presented in figure 3.2. It summarizes the whole methodology of this research.

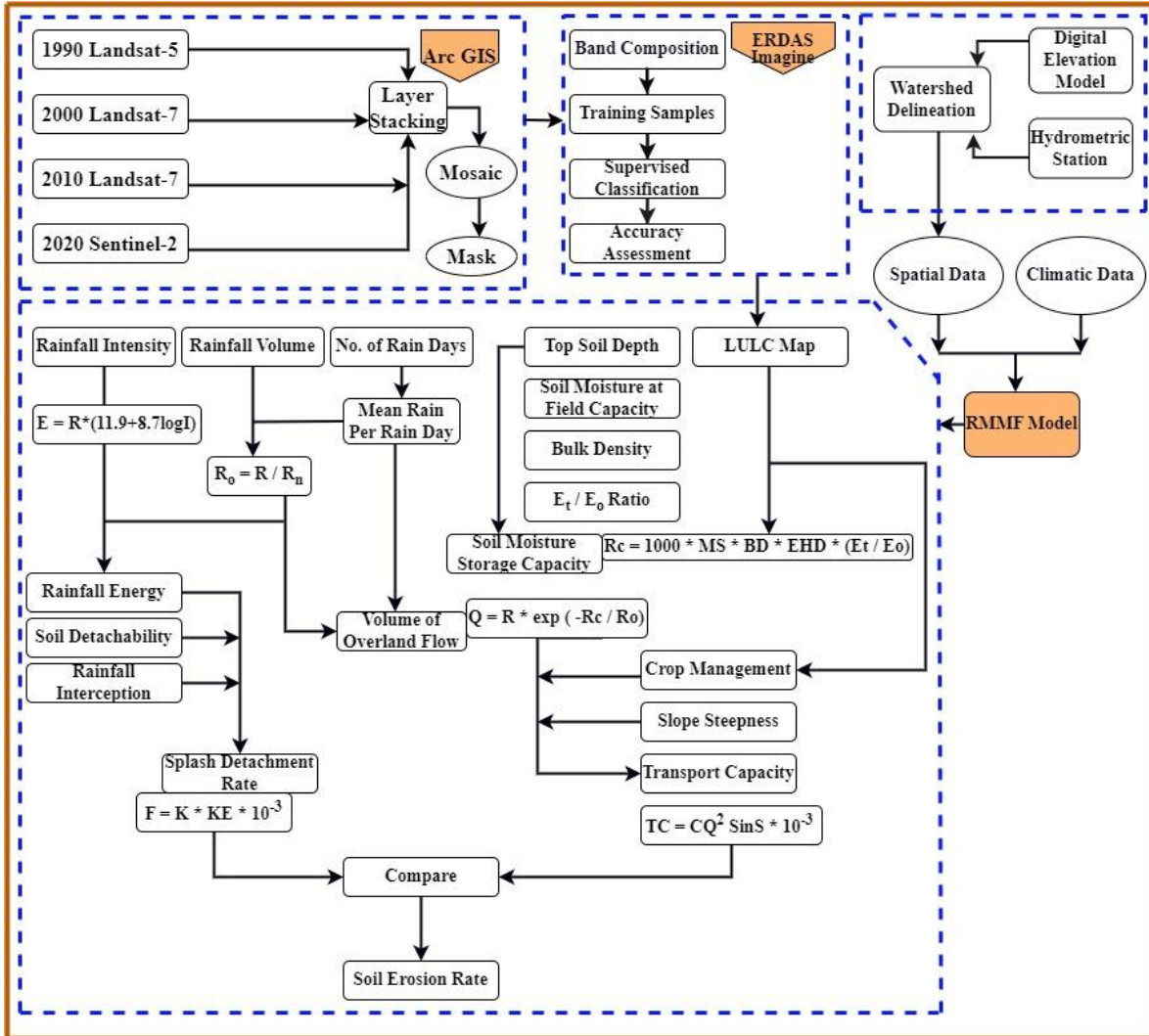


Figure 3.2: Methodology flowchart

3.6 Description of Soil Map

The Soan River catchment is characterized by two soil groups, one has moderately high (C) and the other has very high runoff potential (D) (Figure 3.3).

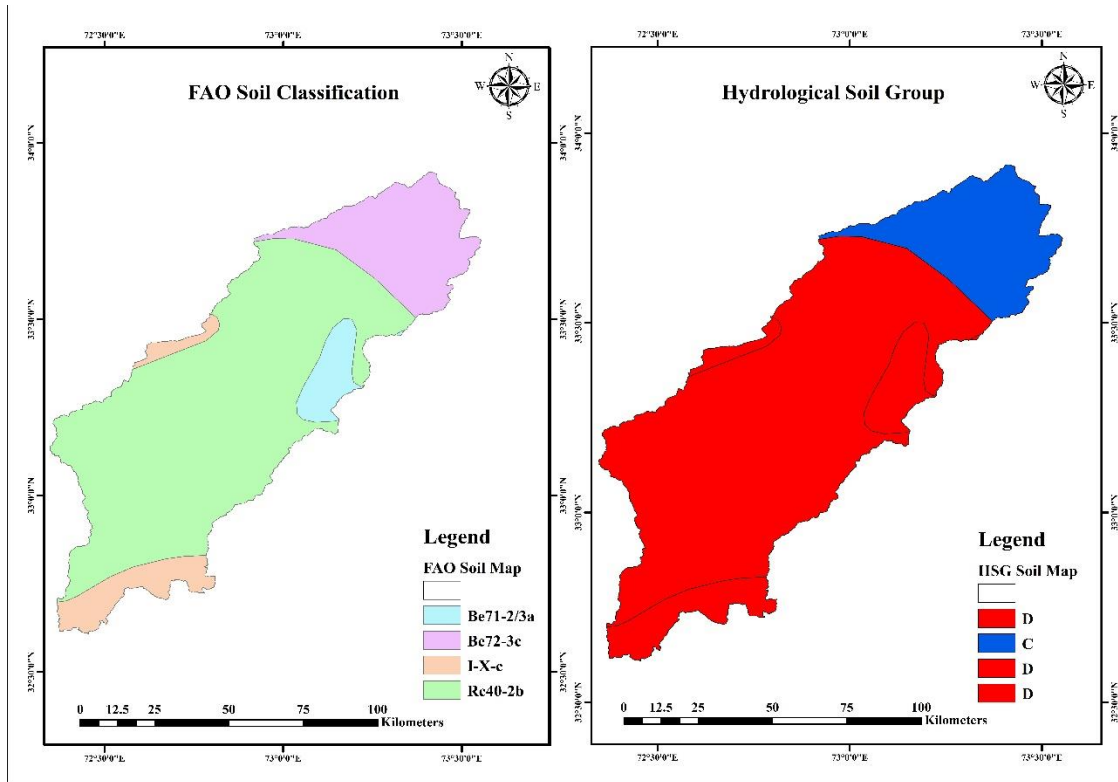


Figure 3.3: FAO soil classification of Soan catchment & Hydrological Soil Group

3.7 Assessment of Historical LULC Change

Four satellite images were used for the assessment of LULC: Sentinel-2A 2020, Landsat-ETM+ 2010, Landsat-7 ETM+ 2000, and Landsat-5 TM 1990. The Landsat images each had a spatial resolution of 30 meters, while the Sentinel picture had a resolution of 10 meters. Due to the scan line corrector failing, Landsat 7 ETM+ includes the errors of scan line that were acquired after 31-05-2003. (SLC). Therefore, the Landsat tool is used to rectify these scan line errors first. After this procedure, the following phase involves supervised categorization using Imagine ERDAS. More than 500 training samples were gathered for this purpose in order to build signature files, which are then utilized to carry out supervised classification using the "Maximum Likelihood Classification (MLC)" technique.

The following step after a successful classification is to verify the image's correctness. Data from the ground is needed for it. To achieve this, one hundred sampling points for each type of Land Use and Land Cover (LULC) were gathered utilizing Google Earth

maps. ERDAS software automatically computes the kappa coefficient, user's accuracy, producer's accuracy, and overall accuracy after conducting ground truthing.

3.8 Accuracy Assessment of Classified Images

After classification has been completed, accuracy evaluation is a critical step. It is done to evaluate how accurately a classified image is described. The matrix technique is the most commonly used method for evaluation, and it is also used in the current study. The values of the categorized data are displayed in rows and the references are displayed in columns in a confusion matrix. Once the confusion matrix is created, it is simple to determine the producer's accuracy, overall accuracy, user's accuracy, omission error, Kappa statistics, and commission error.

3.8.1 Overall Accuracy

One of the essential steps in performing an accuracy assessment is to determine overall accuracy. It is calculated by dividing the total number of designated training pixels by the count of pixels that were successfully classified.

$$\text{Overall Accuracy (\%)} = OA = 100 \sum C / \sum T \quad 3.16$$

Where $\sum C$ is the sum of successfully classified sample and $\sum T$ is the total number of training samples that have been defined.

3.8.2 Producer's Accuracy

It is determined by dividing the total number of reference pixels by the number of pixels that were correctly classified in one class. It is determined by producer's precision, whether the specified area is classified accurately or not. It also takes into consideration the ratio of ground characteristics that were observed but not marked on the map, which is also known as omission error. The accuracy of the producer decreases as the number of omission errors increases.

$$\text{Producers accuracy (\%)} = 100 (\%) - \text{Error of omission (\%)} \quad 3.17$$

3.8.3 User's Accuracy

The User's accuracy can be determined by dividing the number of pixels correctly classified in a class by the total number of pixels assigned to that class. Thus, the accuracy of the user is a gauge of accuracy of the map. It shows the user how accurately the map depicts what is really happening on the ground.

$$\text{Users Accuracy (\%)} = 100 (\%) - \text{Error of Commission (\%)} \quad 3.18$$

3.8.4 Kappa Coefficient

The Kappa coefficient is utilized to assess the general concordance of a matrix. Instead of the complete accuracy the focus is on proportion of the total number of pixels that corresponds to the sum of diagonal values in the matrix. Additionally, the Kappa coefficient considers the non-diagonal components as well.

$$\frac{N \sum_{i=1}^r X_{ii} - \sum_{i=1}^r (X_{i=1} + X_i)}{N^2 - \sum_{i=1}^r (X_{i+1} + X_i)} \quad 3.19$$

Where r denotes the number of columns and rows in error matrix, total number of matrix are denoted by N, X_{ii} is equal to observation in column i and, row i and X_i is equal to marginal total of column i.

Table 3.4: Description of Kappa coefficient range and interpretation

Kappa Coefficient	Interpretation
<0	Poor Agreement
0.0- 0.20	Slight Agreement
0.20- 0.40	Fair Agreement
0.40- 0.60	Moderate Agreement
0.60- 0.80	Substantial Agreement
0.80- 1.0	Almost Perfect Agreement

Results and Discussions

This chapter contains LULC results of 1990, 2000, 2010, and 2020. Also contains results of soil erosion estimation by using RMMF Model. The detailed results are discussed in this chapter.

4.1 Land Use / Land Cover Maps

LULC maps are classified into five types, namely water bodies, agricultural land, forest areas, barren area and built-up land. Figure 4.1 & Figure 4.2 depict the maps from 1990, 2000, 2010, and 2020, which show an increase in built-up and agricultural lands while decrease in forest and barren lands.

4.2 Accuracy Assessment

The accuracy of classified imageries is assessed in order to estimate their dependability. The accuracy assessment for the 1990, 2000, 2010 and 2020 classified photos is carried out in this study employing a total of more than 500 ground truthing sites using Google Earth Map for each image.

During the accuracy evaluation, the quality of the categorized images is assessed using a confusion matrix. Using the Google Earth maps and mosaicked satellite data as references for the categorization maps, spots were randomly selected and compared to them. With 100 sample points for each class, 500 ground truthing points were chosen for each classed image from 1990, 2000, 2010, and 2020 to validate the data. Results (Table 4.1) show that for maps from 1990, 2000, 2010, and 2020, the average kappa index and overall accuracy were 0.79, 0.81, 0.82, and 0.84, respectively, or 83.8%, 85.2%, 85.88%, and 87.8%. The accuracy of the producer ranges from 75% to 94%, whereas that of the user ranges from 79% to 97%. Landis and Monserud claim that Kappa coefficients between 0.70 and 0.85 are excellent predictors of the categorized image (Landis & Koch,

1977) (Monserud & Leemans, 1992). As a result, the validation points demonstrated that the classified image and the actual situation had an excellent correlation.

Table 4.1: Accuracy Assessment of Historical LULC's

LULC Classes	1990		2000		2010		2020	
	U	P	U	P	U	P	U	P
Water	97.00	100.00	95.00	100.00	96.00	100.00	98.00	100.00
Agriculture	82.00	82.00	79.00	84.04	85.00	80.95	89.00	84.76
Forest	92.00	92.93	98.00	80.99	94.00	94.95	100.00	93.46
Barren	85.00	69.11	74.00	68.52	85.00	64.89	96.00	76.89
Built-up	80.00	98.77	80.00	97.56	66.00	95.65	67.00	98.53
Overall Accuracy	83.80		85.20		85.80		87.20	
Kapa Coefficient	0.7975		0.8150		0.8225		0.8475	

4.3 Spatiotemporal Variation in LULC

For the years 1990, 2000, 2010, and 2020, depicts the comparable areas of each class of the supervised classified LULC. The Soan Catchment **Table 4.2** LULC maps from 1990, 2000, 2010, and 2020 were examined to look at LULC changes and their impact on the erosion of soil of the catchment. Overall, it was discovered that the area is experiencing an increase in human influence as a result of machine agriculture's expansion, unchecked infrastructure development, as well as a decline in forested and arid areas. Figure 4.1 shows the spatiotemporal pattern of LULC change in the Soan catchment from 1990 to 2020. It proves that arid terrain was turned into agricultural land in the downstream regions. The upstream area's built-up areas expanded greatly in the interim by turning agricultural, arid, and forested lands into impermeable terrain. Agricultural land experienced the greatest variation between all LULC types, rising by 35.44% since 1990. The LULC shift is however insignificant when compared to the catchment overall geographic area. This suggests that the sub-basin level of the LULC alteration has been more dramatic than the catchment level. Positive changes in one LULC class have more

than offset negative changes in another LULC class at the catchment level. Agricultural activity, for instance, has increased in the middle and downstream regions while declining in upstream parts due to the conversion of agricultural land into built-up areas.

Table 4.2 displays the historical LULC variance from 1990 to 2020. It is distinguished by the shift to arid land, which lost a total of 3054.14 km² before being replaced by built-up areas and agricultural land. Water changed the least, whereas agricultural land experienced an increasing trend, adding 2318.75 km². By 2020, built-up land also increased steadily to a size of roughly 1096.62 km². Agricultural and built-up areas have seen improvements. At the same time, forest and arid lands will change into different LULC types (Tariq et al. 2020). In the counties of Attock, Chakwal, and twin cities, urban sprawl may be to blame for the loss of forest and arid terrain.

Table 4.2: LULC coverage in Soan River catchment

LULC	1990		2000		2010		2020	
	Km ²	%	Km ²	%	Km ²	%	Km ²	%
Water	35.91	0.55	45.77	0.70	51.35	0.78	71.45	1.09
Agriculture	1178.57	18.01	2128.18	32.53	3281.13	50.15	3497.32	53.45
Forest	1221.88	18.68	1126.53	17.22	1116.24	17.06	990.02	15.13
Barren Land	3940.73	60.24	3075.34	47.01	1850.54	28.29	886.59	13.55
Built-up	164.91	2.52	166.18	2.54	242.74	3.71	1096.62	16.76

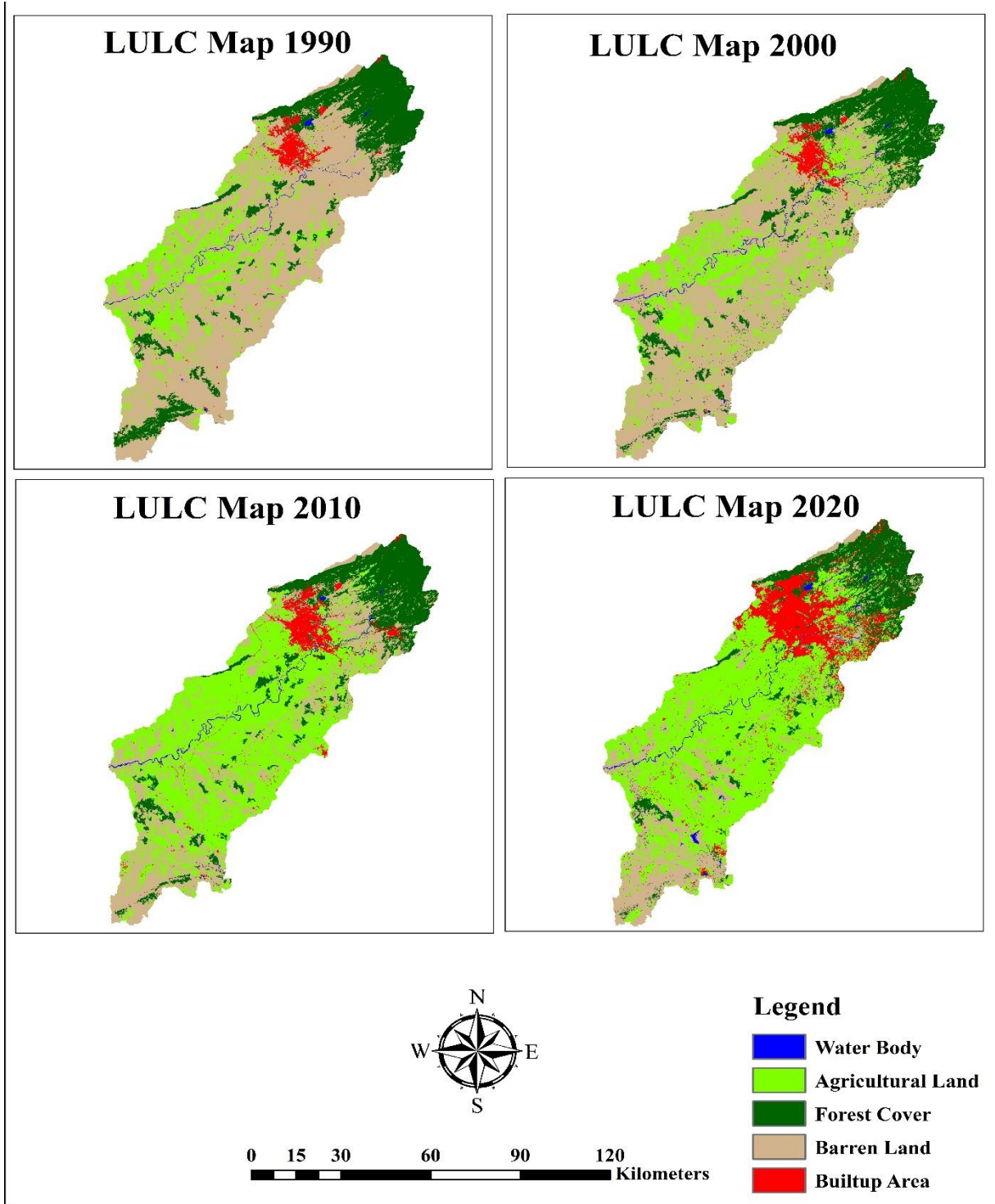


Figure 4.1: LULC map of Soan River Catchment

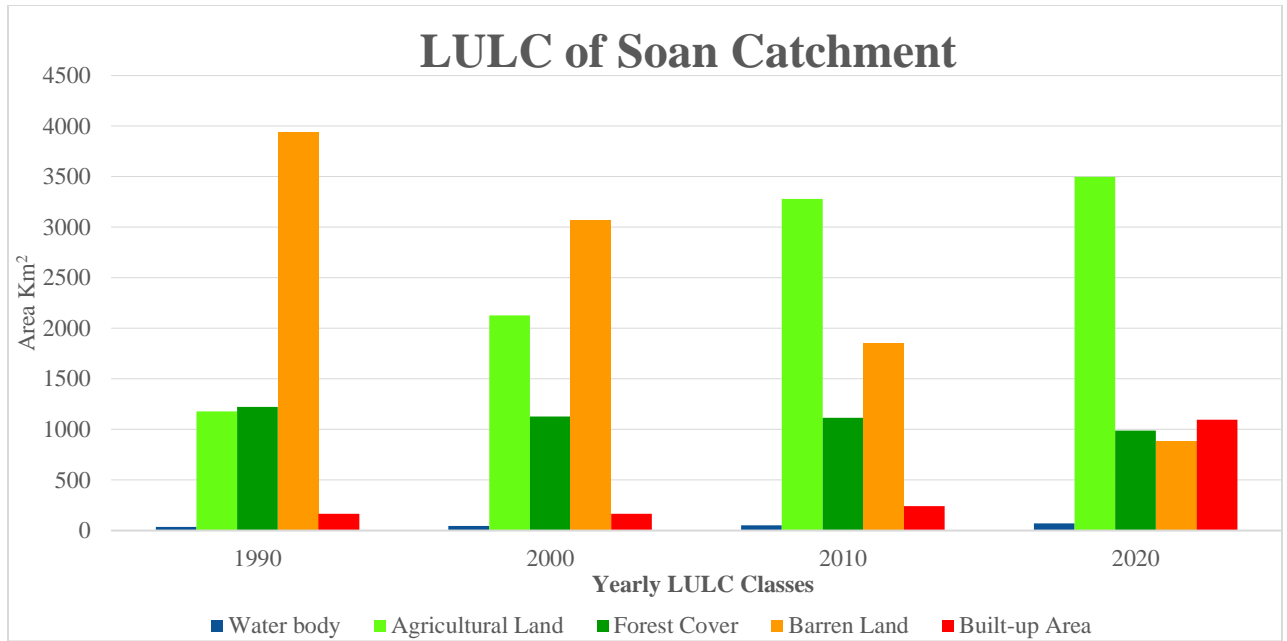


Figure 4.2: LULC map of Soan River Catchment

4.4 Revised Morgan-Morgan-Finney Model

Revised Morgan-Morgan-Finney model was used to estimate the soil erosion of Soan River catchment, and the results are given below;

4.4.1 Rainfall Energy

By using the different values of mean annual rainfall (R) fig.4.3 and rainfall interception coefficient (A), effective rainfall (ER) shown in fig.4.4 was calculated. Based on a literature review (Finney, 1984), “A” shown in fig.4.5 was calculated using the basin's land-use delineation. The process involved determining an empirical value for each distinct type of land cover that was observed and then utilizing these values of CC factor to calculate the DT and LD components based on the assigned values. As a function of the KE and PH, the corresponding kinetic energies were calculated. Where KE (DT) was calculated by taking the value of intensity of rainfall ($I = 25 \text{ mm/hr.}$) for tropical climate of basin. Ultimately, the complete kinetic energy of precipitation (KE) was computed by combining the two components of kinetic energy. Vegetation has essential role in the prevention of soil erosion as forest cover has highest values of PH, CC, GC, EHD, E_t / E_o and lowest C factor. PH, A, E_t / E_o CC, and C are above-ground components (canopy)

while EHD and GC (Effective hydrologic depth & ground cover) are on or below ground components. Regions characterized by agricultural landuse with shorter canopy heights and denser ground cover exhibits reduced level of leaf drainage and kinetic energy of leaf drainage. Conversely, these same areas experience elevated values of direct throughfall and kinetic energy of direct throughfall due to unobstructed rainfall reaching the ground surface.

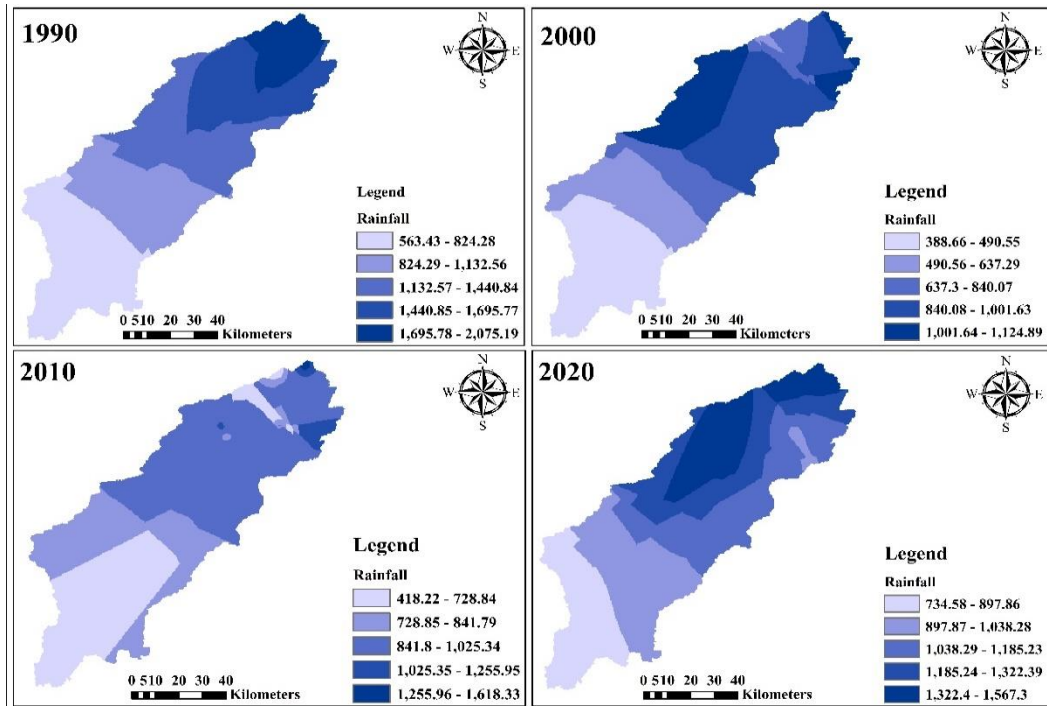


Figure 4.3: Annual rainfall map of Soan River Catchment (1990, 2000, 2010 and 2020)

4.4.2 Effective runoff

The parameters of precipitation were taken into account to estimate the annual runoff based on R_c . Parameters of soil (MS, BD, and EHD) and actual to potential Evapotranspiration ratio (E_t / E_o) were used to calculate R_c . Guide values for EHD, MS and BD were given in revised version of Morgan-Morgan-Finney model (Finney, 1984). By opening soil map in Arc GIS and right clicking, option for attribute table shows. By clicking that option attribute table opens, where the values of above parameters were edited. Then in Arc toolbox “Feature to Raster” tool was used to draw the raster of above parameters. Division of mean annual rainfall by the number of rainy days was done to calculate the value of R_o .

The watershed's lowlands and hilly regions have the greatest MS values, which indicate moderately fine and fine soils, respectively. The northern region of the catchment, where peak values were found for both of R_C as well as soil parameters. In terms of Q , the low-class values were more prevalent throughout the catchment, whereas the high class values were found in a small number of low R_C locations

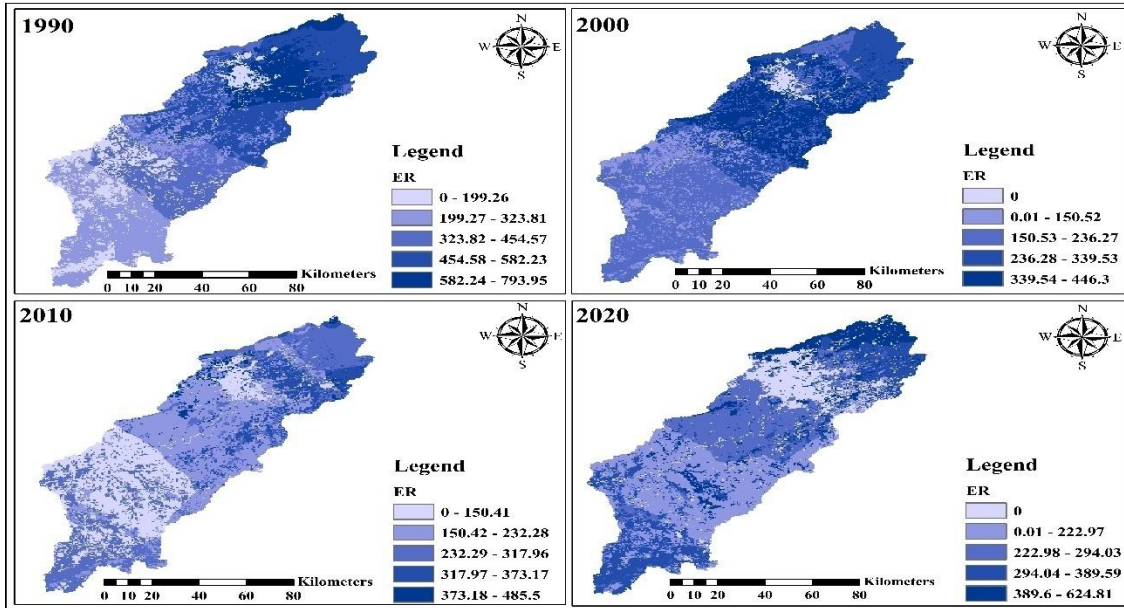


Figure 4.4: Effective rainfall map of Soan River Catchment (1990, 2000, 2010 and 2020)

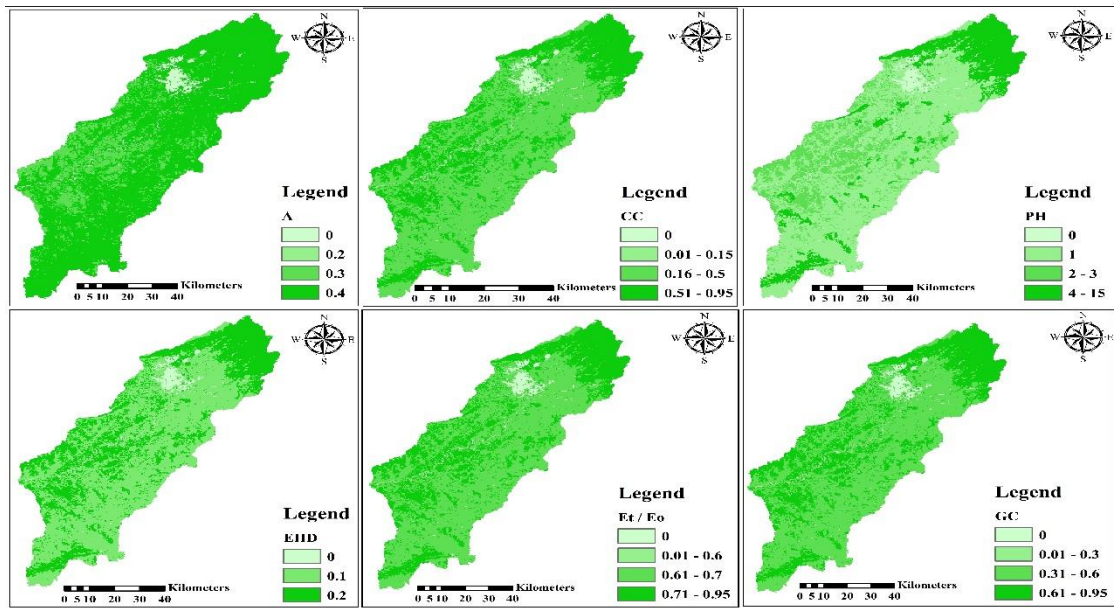


Figure 4.5: Landuse/landcover parameters: rainfall interception coefficient, A (%); canopy cover, CC (%); canopy height, PH (m), effective hydrological depth of soil, EHD (m); actual to potential evapotranspiration, E_t/E_o (%) and ground cover, GC (%)

4.4.3 Soil particle detachment by raindrop impact

Detachment of soil particle by the impact of raindrop shown in fig 4.8 was calculated by multiplying kinetic energy shown in fig 4.6 and K values shown in fig 4.7. The values of kinetic energy by leaf drainage and direct throughfall were added to generate the raster map of kinetic energy. K was calculated by adding different values of soil detachability index in the soil map of catchment in “ARC GIS”. “Feature to raster” tool was used to draw the raster of soil detachability index (K) of study area. As already discussed, KE is tends to be higher in lowland areas where vegetation cover is short and dense, allowing greater throughfall volume and intensity of rainfall to reach the surface of soil without obstruction. The most erodible soils are those with the highest K values. The aforementioned values indicating the erodibility to detachment, which suggest the moderate potential for runoff, were observed in soil belonging to the medium and moderate fine textural classes. These type of soil are predominantly located in lowlands areas of the basin with less vegetation. This is according to the classification map approximation (mainly on mountainous areas of extended land cover). Overall, K is more intense in places with mild morphology in the classification map approach, largely reflecting the spatial distribution of KE. Short and dense vegetation, regional characteristics of catchment, and perpendicular raindrop impact on the surface of soil, which concentrates their energy are some factors which can be used to explain the aforementioned statement. Raindrops collide with the ground at an angle in hilly and mountainous places, suggesting that the energy of raindrop impact decreased on steep morphology. Nevertheless, on flat terrain, the net and transported volumes of detached soil are about identical, whereas on sloped surfaces, a greater number of removed soil particles results in a downward slope.

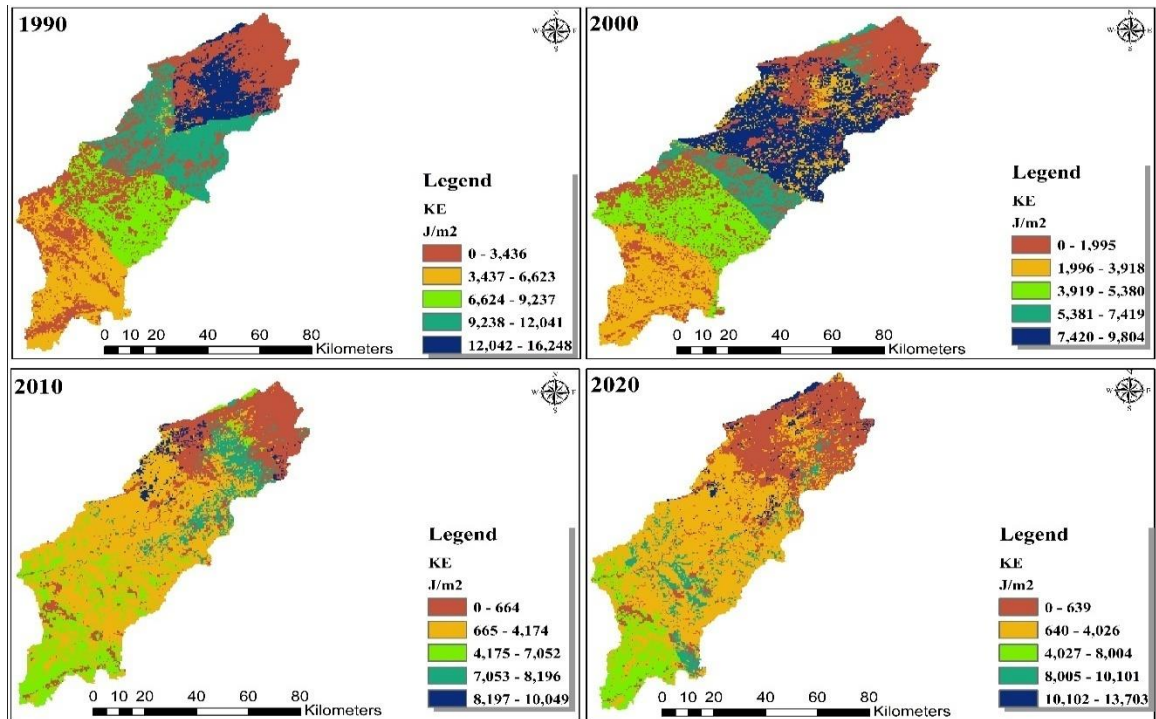


Figure 4.6: Kinetic Energy

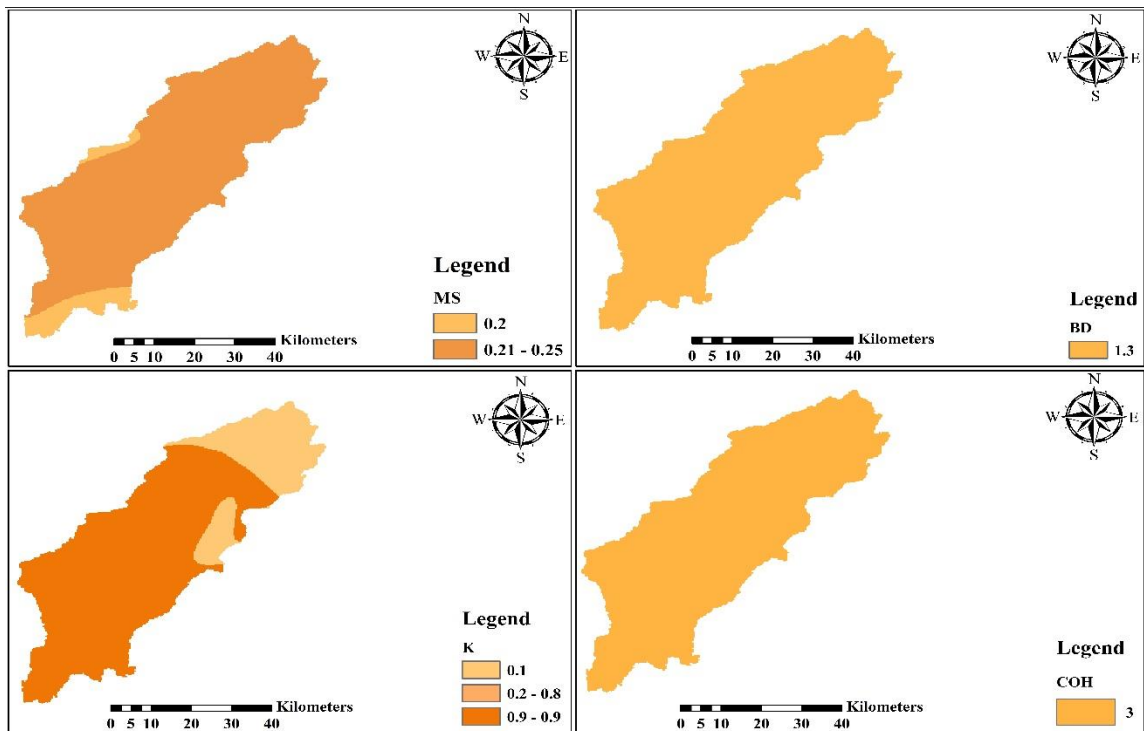


Figure 4.7: Soil Parameters: moisture content at field capacity or 1/3 bar tension, MS (% WW⁻¹); bulk density of the top layer, BD (Mgm⁻³); detachability index, K (gj⁻¹) and cohesion, COH (Kpa)

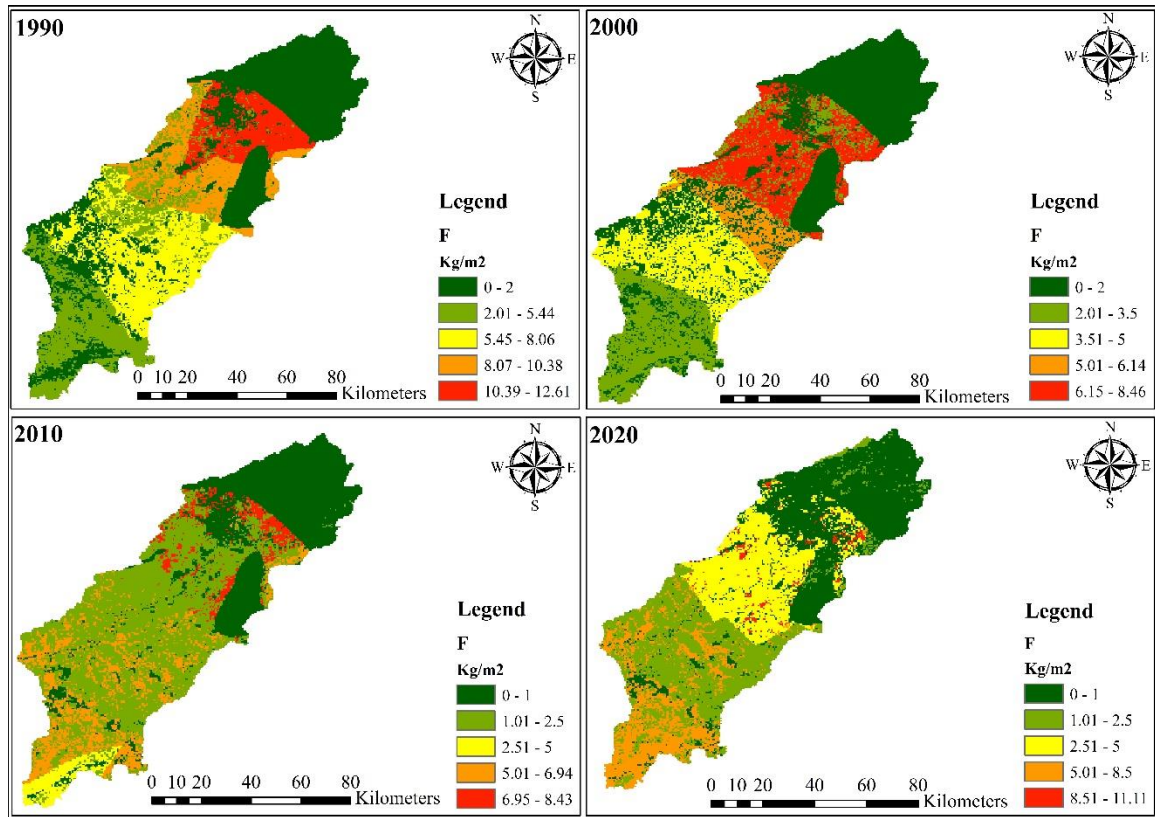


Figure 4.8: Soil particle detachment by raindrop impact, F (kgm^{-2})

4.4.4 Soil particle detachment by runoff

Overland flow, Slope, Ground Cover, and Z factors were used to calculate the value of detachment of soil particle by runoff (H) shown in fig 4.9. As told earlier in equation 3.12, to calculate the value of Z, COH value was multiplied with 0.5 and then divide 1 by that value will gives you the value of Z. Slope (S°) of catchment was obtained from the digital elevation model (DEM). As COH is constant and the entire basin has same value, which is “3”, and dominate the whole basin area, suggesting that the basin is actually effected by precipitation as compared to overland flow. This is primarily because of the dense vegetation that covers the sloppy, hilly, and mountainous regions, which inhibits surface runoff's ability to separate particles. It should be emphasized, in these areas, the rate of runoff detachment was anticipated to be higher because the volume and speed of overland flow increase with increasing slope steepness, and because the soil would be finer and saturated rapidly, may favored surface runoff.

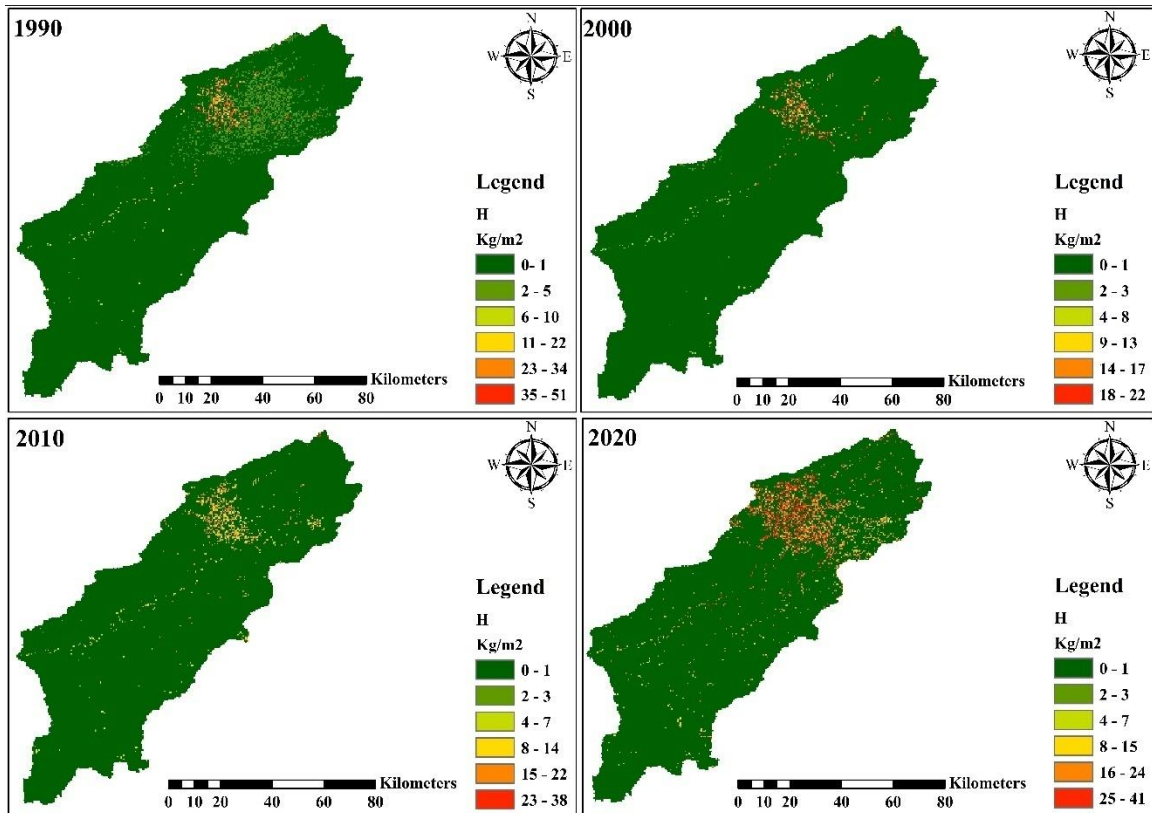


Figure 4.9: Soil particle detachment by runoff, H (kgm^{-2})

4.4.5 Transport capacity of runoff

Most of the basin area has low transport capacity. As shown in fig 4.10, most of the area lies in the range of (0-5 kg/m^2). Some of the areas of Islamabad and Rawalpindi are also lies under the higher transport capacity range because of urbanization and deforestation, these areas generates more overland flow as well as the higher velocity and more slope as compared to other areas of downstream. While the areas where transport capacity of sediment is low is due to the less slope and dense cover of vegetation. Map depict that in 1990, most of the area of Islamabad and Rawalpindi lies under the range of 0-20 kg/m^2 but in 2020 these areas and the some of the area of Murree lies under the range of 20-70 kg/m^2 . Low TC additionally denotes constrained movement, resulting in high deposition rates of detached particles that are unable to exit the basin.

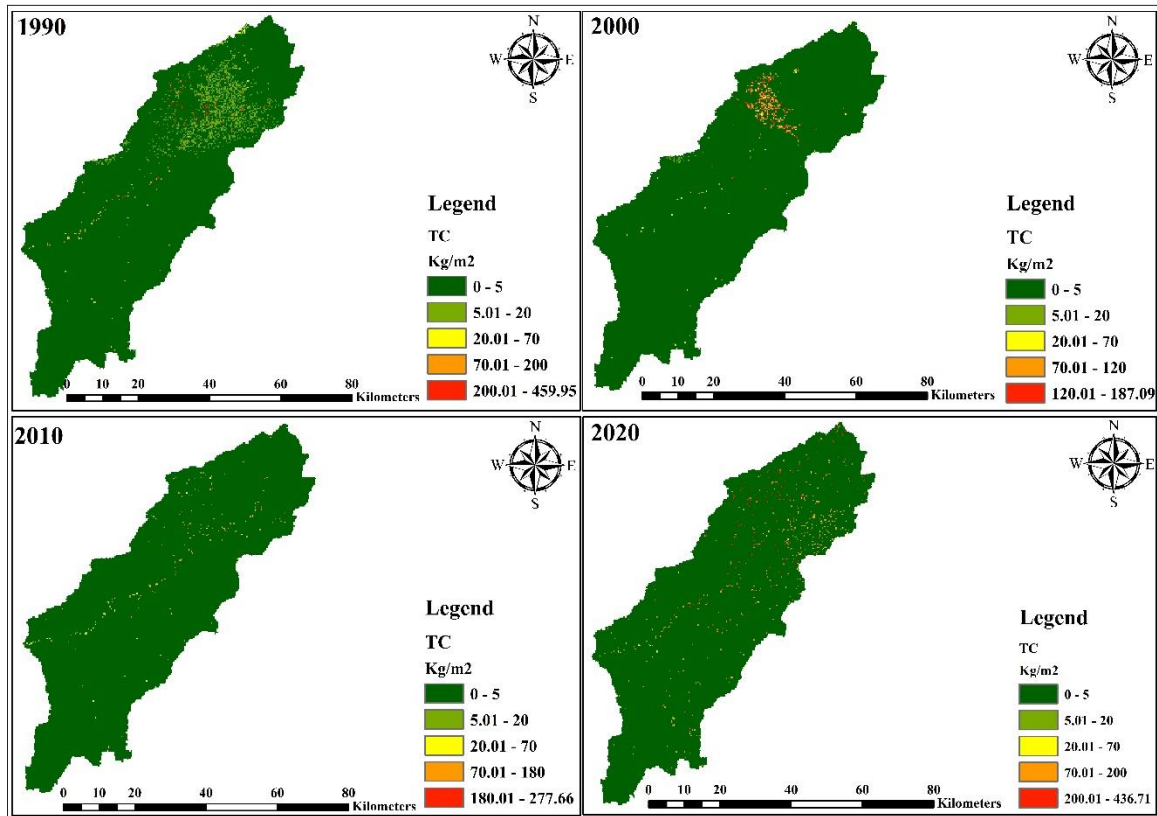


Figure 4.10: Transport Capacity of runoff (Kg m^{-2})

4.4.6 Erosion estimation

When we add erosion due to raindrop impact and runoff, fig. 4.11 shows that, most of the areas of Islamabad, Rawalpindi, Chakwal and Attock in 1990 has erosion range of 6-15 kg/m^2 which is almost 60 to 150 $\text{tha}^{-1}\text{year}^{-1}$, but one can see in 2000, area of Chakwal has erosion range of 0-5 Kg/m^2 or 0-50 $\text{tha}^{-1}\text{year}^{-1}$ and other areas were still under the same range of erosion as it was in 1990. In 2010 almost all of those areas which were in 6-15 kg/m^2 range, are in 0-5 kg/m^2 range of erosion. But in 2020 as the above mentioned areas has erosion range mostly between 0-50 $\text{tha}^{-1}\text{year}^{-1}$ and some areas of lowland are lies under the range of 50 to 150 $\text{tha}^{-1}\text{year}^{-1}$ as well as areas of Islamabad, Rawalpindi and Murree has erosion rate of above 150 $\text{tha}^{-1}\text{year}^{-1}$ which is due to the human interference. Construction and deforestation has really activated the erosion, and severity of erosion has arisen in these areas.

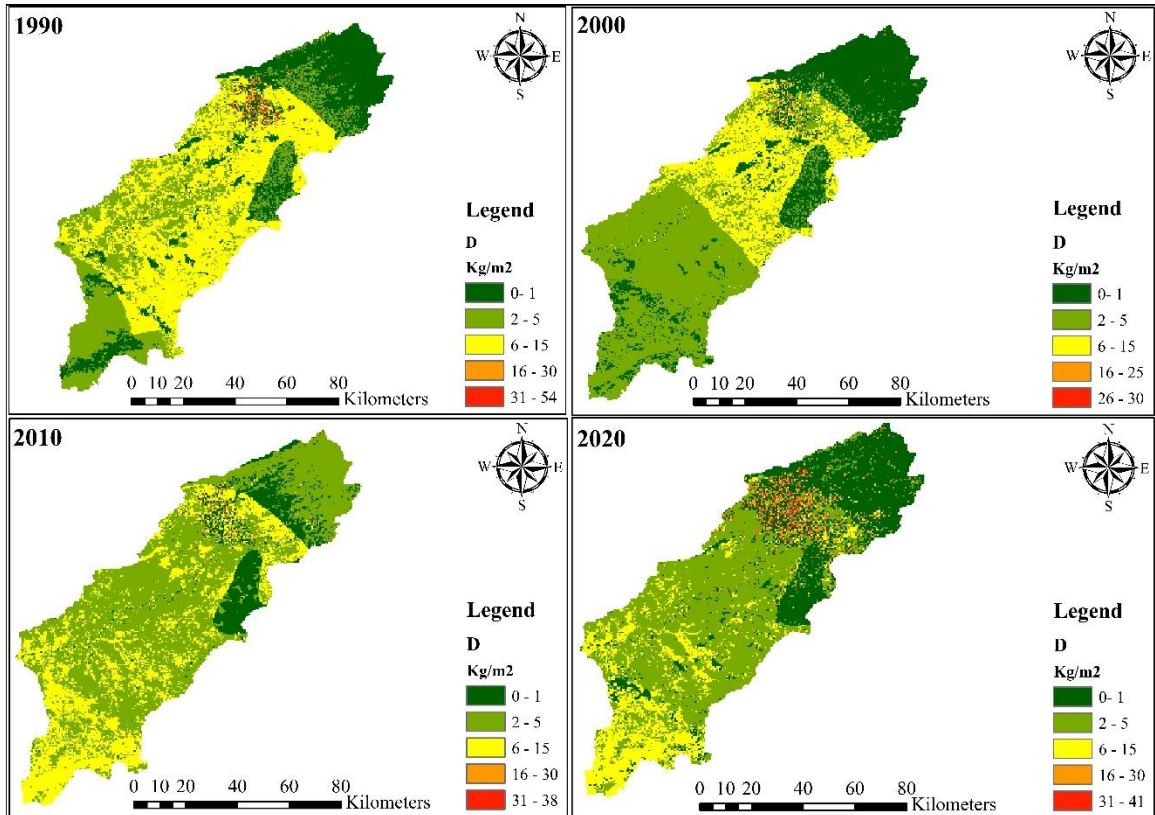


Figure 4.11: Total annual detachment rate of soil, D (kgm^{-2})

Table 4.3: Area vs range of erosion.

1990			2000		2010		2020	
Polygon	Area Km^2	Erosion Kg/m^2	Area Km^2	Erosion Kg/m^2	Area Km^2	Erosion Kg/m^2	Area Km^2	Erosion Kg/m^2
1	1495.9	0-5	1480.66	0-0.59	3884.3	0-2	2218.35	0-2
2	968.73	5-10	869.09	0.59-1.61	1153.88	2-5	2749.34	2-5
3	456.52	10-15	456.16	1.61-2.67	1246.54	5-10	1094.21	5-10
4	1183.64	15-20	1245.89	2.67-3.76	66.17	10-15	70.62	10-15
5	1046.75	20-25	833.16	3.76-4.94	51.19	15-20	87.33	15-20
6	1036.78	25-30	405.35	4.94-6.79	11.32	20-25	101.13	20-25
7	170.28	30-37	1075.46	6.79-12.91	2.49	25-30	63.85	25-30
8	62.05	37-54.04	67.72	12.91-29.63	0.14	30-38.37	54.69	30-41.09

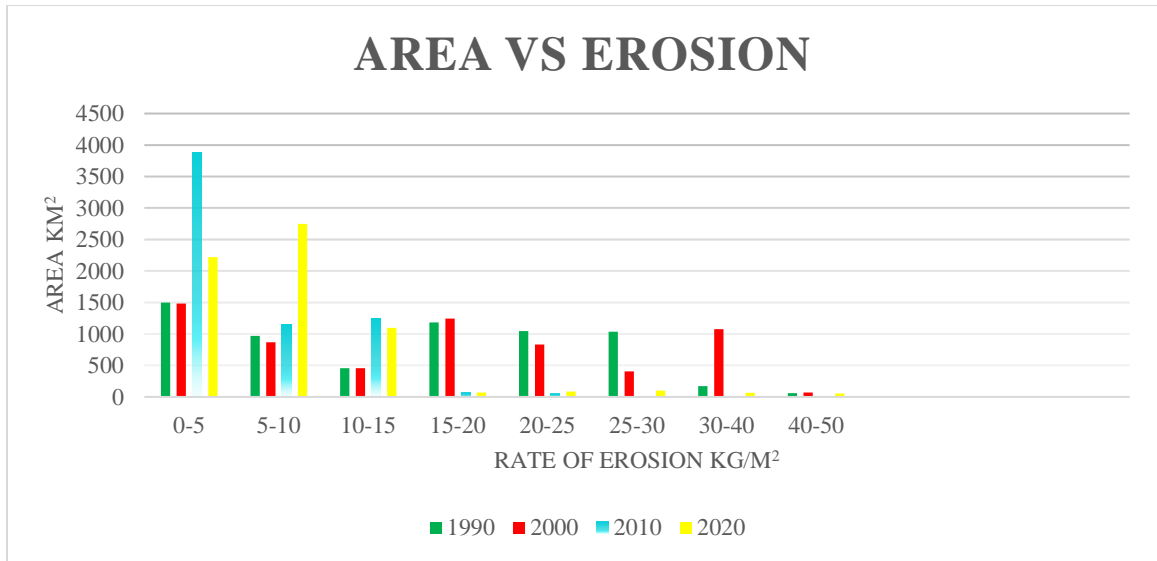


Figure 4.13: Area (Km2) vs Total annual detachment rate of soil (Kg/m²)

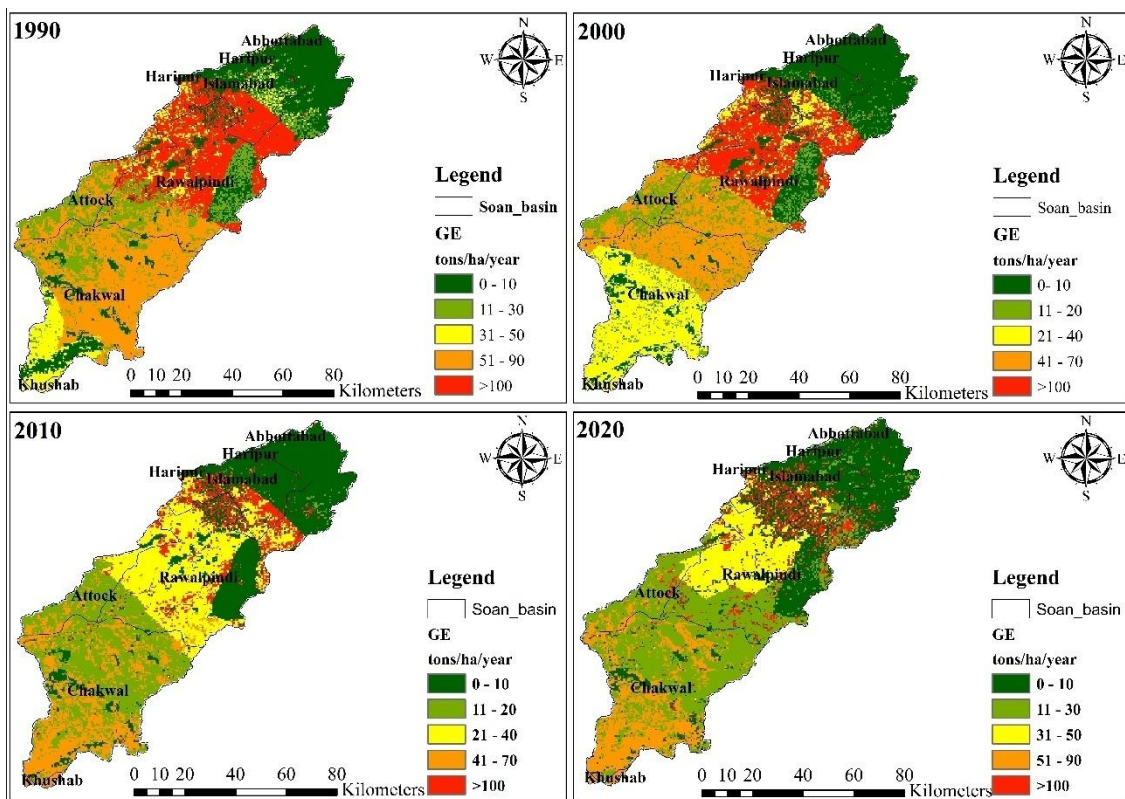


Figure 4.12: Gross Erosion, GE (t/ha/year)

Conclusions & Recommendations

5.1 Conclusions

This study assessed soil erosion for the Soan River catchment. The results showed that the Soan River catchment has areas which lie under high-risk zone of soil erosion.

Results for LULC shows that in 1990 Barren land, has an area of 3940.73 km², and reduced to 886.59 Km² in 2020. Also, Forest area was 1221.88 Km² in 1990 and reduced to 990.02 km². But agricultural and built-up area has a significant increase in 2020 as compared to 1990, which shows that barren and forest land was converted into agricultural and built-up land.

In 1990 and 2000, areas of Rawalpindi, Islamabad and a part of Haripur district were under high risk of erosion. As maps suggest that most of these areas have erosion higher than 100 ton/ha/year. As one can see in LULC maps of 1990 and 2000, areas having soil erosion greater than 100 ton/ha/year have less vegetation and most of the area lies in barren land class. In 2010 and 2020, most of the barren land was converted in to agricultural and built-up area.

According to (Ahsan, 2008) the annual average soil loss for the Soan river basin was 3541 tons km⁻² year⁻¹. He also concluded that the highest soil loss was 6341 tons km⁻² year⁻¹ in barren land and lowest soil loss was 1876 tons km⁻² year⁻¹ in cropland. The risk of soil erosion in Soan River Basin was assessed by (Ashraf, 2020) using Revised Universal Soil loss equation coupled with geo informatic techniques. The results of his study reveals that about 6.5 % area of Soan River Basin lies in High (where soil loss is 30-100 tons ha⁻¹ year⁻¹) to very high (where soil loss is more than 100 tons ha⁻¹ year⁻¹) risk zone and 12.9 % area of the basin lies in medium risk zone, where soil loss is 10-30 tons ha⁻¹ year⁻¹ . GIS based risk modelling of soil erosion under different land use scenarios of Simly watershed was done by (Muhammad Khubaib Abuzar, 2018) using Revised Universal Soil Loss Equation. Their study reveals that normal rate of 14 tons ha⁻¹

year⁻¹ soil erosion in the Simly Watershed. They used zonal statistics of ArcGIS for the calculations.

The study's findings make it abundantly evident that this model can be used for both qualitative and quantitative assessments of soil erosion intensity for conservation management.

Data from Land Sat and Sentinel-2A is useful for analyzing land use. For this investigation, useful and crucial elements like C and P have been provided using multi temporal, multi sensor, and multispectral remote sensing data. Because crop cover is a potent tool for reducing the direct effects of rainfall on soil particles.

5.2 Future Recommendations

- It is advised that all barren land in the Soan River catchment be transformed into agricultural or forest plantations using appropriate land reclamation techniques
- The following structures for soil and water conservation should be considered: Agriculture on slopes steeper than 10° greatly increases erosion. Strip cropping is preferable if changing the land's usage is not an option
- Socioeconomic variables should be assessed prior to developing any soil and water control plans
- To determine the impact of soil erosion on dams and other hydrologic infrastructure, a study on sediment transport using the SWAT model is recommended in the future

References

- Abijith, D., Saravanan, S., Singh, L., Jennifer, J. J., Saranya, T., & Parthasarathy, K. (2020). GIS-based multi-criteria analysis for identification of potential groundwater recharge zones-a case study from Ponnaniyar watershed, Tamil Nadu, India. *HydroResearch*, 3, 1-14.
- Abuzar, M. K., Shakir, U., Ashraf, M. A., Mukhtar, R., Khan, S., Shaista, S., & Pasha, A. R. (2018). GIS based risk modeling of soil erosion under different scenarios of land use change in Simly watershed of Pakistan. *Journal of Himalayan Earth Sciences*, 51(2A), 132-143.
- Akinyemi, F. O. (2021). Vegetation trends, drought severity and land use-land cover change during the growing season in semi-arid contexts. *Remote sensing*, 13(5), 836.
- Alam, S., Fatima, A., & Butt, M. S. (2007). Sustainable development in Pakistan in the context of energy consumption demand and environmental degradation. *Journal of Asian Economics*, 18(5), 825-837.
- Alexakis, D. D., Hadjimitsis, D. G., & Agapiou, A. (2013). Integrated use of remote sensing, GIS and precipitation data for the assessment of soil erosion rate in the catchment area of “Yialias” in Cyprus. *Atmospheric Research*, 131, 108-124.
- Ashiagbor, G., Forkuo, E. K., Laari, P., & Aabeyir, R. (2013). Modeling soil erosion using RUSLE and GIS tools. *Int J Remote Sens Geosci*, 2(4), 1-17.
- Aticho, A. (2013). Evaluating organic carbon storage capacity of forest soil: Case study in Kafa Zone Bita District, Southwestern Ethiopia. *American Eurasian Journal of Agriculture and Environmental Science*, 13(1), 95-100.
- Bagley, J. E., Desai, A. R., Dirmeyer, P. A., & Foley, J. A. (2012). Effects of land cover change on moisture availability and potential crop yield in the world's breadbaskets. *Environmental Research Letters*, 7(1), 014009.
- Bagley, J. E., Desai, A. R., Harding, K. J., Snyder, P. K., & Foley, J. A. (2014). Drought and deforestation: has land cover change influenced recent precipitation extremes in the Amazon? *Journal of Climate*, 27(1), 345-361.
- Bai, Y., Ouyang, Z., Zheng, H., Li, X., Zhuang, C., & Jiang, B. (2012). Modeling soil conservation, water conservation and their tradeoffs: a case study in Beijing. *Journal of Environmental Sciences*, 24(3), 419-426.
- Bai, Z. G., Dent, D. L., Olsson, L., & Schaepman, M. E. (2008). Proxy global assessment of land degradation. *Soil use and management*, 24(3), 223-234.
- Baig, M. B., Shahid, S. A., & Straquadine, G. S. (2013). Making rainfed agriculture sustainable through environmental friendly technologies in Pakistan: A review. *International Soil and Water Conservation Research*, 1(2), 36-52.
- Baliani, A., & Vaezi, A. (2017). The susceptibility of different texture soils to splash erosion under different rainfall intensity and antecedent water content. *Journal of Water and Soil Conservation*, 24(2), 67-85.
- Berhe, A. A., Harte, J., Harden, J. W., & Torn, M. S. (2007). The significance of the erosion-induced terrestrial carbon sink. *BioScience*, 57(4), 337-346.
- Blanco, H., & Lal, R. (2008). *Principles of soil conservation and management* (Vol. 167169). Springer New York.

- Boardman, J., Vandaele, K., Evans, R., & Foster, I. D. (2019). Off-site impacts of soil erosion and runoff: Why connectivity is more important than erosion rates. *Soil use and management*, 35(2), 245-256.
- Braimoh, A. K., & Osaki, M. (2010). Land-use change and environmental sustainability. *Sustainability Science*, 5, 5-7.
- Breshears, D. D., Whicker, J. J., Johansen, M. P., & Pinder, J. E. (2003). Wind and water erosion and transport in semi-arid shrubland, grassland and forest ecosystems: Quantifying dominance of horizontal wind-driven transport. *Earth Surface Processes and Landforms: The Journal of the British Geomorphological Research Group*, 28(11), 1189-1209.
- Bringezu, S., Schütz, H., Pengue, W., O'Brien, M., Garcia, F., Sims, R., Howarth, R. W., Kauppi, L., Swilling, M., & Herrick, J. (2014). *Assessing global land use: balancing consumption with sustainable supply*. United Nations Environment Programme Nairobi, Kenya.
- Bruijnzeel, L. A. (2004). Hydrological functions of tropical forests: not seeing the soil for the trees? *Agriculture, Ecosystems & Environment*, 104(1), 185-228.
- Cerdà, A., Daliakopoulos, I. N., Terol, E., Novara, A., Fatahi, Y., Moradi, E., Salvati, L., & Pulido, M. (2021). Long-term monitoring of soil bulk density and erosion rates in two *Prunus Persica* (L) plantations under flood irrigation and glyphosate herbicide treatment in La Ribera district, Spain. *Journal of Environmental Management*, 282, 111965.
- Change, I. C. (2013). The physical science basis. *Contribution of working group I to the fifth assessment report of the intergovernmental panel on climate change, 1535*, 2013.
- Daily, G. C., Matson, P. A., & Vitousek, P. M. (1997). Ecosystem services supplied by soil. *Nature's services: societal dependence on natural ecosystems*, 113-132.
- De Groot, R. S., Wilson, M. A., & Boumans, R. M. (2002). A typology for the classification, description and valuation of ecosystem functions, goods and services. *Ecological economics*, 41(3), 393-408.
- De Roo, A., Wesseling, C., & Ritsema, C. (1996). LISEM: a single-event physically based hydrological and soil erosion model for drainage basins. I: theory, input and output. *Hydrological processes*, 10(8), 1107-1117.
- Denboba, M. A. (2005). *Forest conversion-soil degradation-farmers perception nexus: Implications for sustainable land use in the southwest of Ethiopia* (Vol. 26). Cuvillier Verlag.
- Doran, J. W., & Parkin, T. B. (1994). Defining and assessing soil quality. *Defining soil quality for a sustainable environment*, 35, 1-21.
- Ellis, E. C., Beusen, A. H., & Klein Goldewijk, K. (2020). Anthropogenic biomes: 10,000 BCE to 2015 CE. *Land*, 9(5), 129.
- Foley, J. A., DeFries, R., Asner, G. P., Barford, C., Bonan, G., Carpenter, S. R., Chapin, F. S., Coe, M. T., Daily, G. C., & Gibbs, H. K. (2005). Global consequences of land use. *Science*, 309(5734), 570-574.
- Gabriel, F., & Ayuba, A. (2006). Biodiversity Depletion in Plants: Implications for Ecosystem. *International Journal of Environmental Issues*, 4(1), 104-108.
- Gavriloic, S. (1962). Hispanic American history research opportunities in Yugoslav archives. *Hispanic American historical review*, 42(1), 37-50.

- Gelagay, H. S., & Minale, A. S. (2016). Soil loss estimation using GIS and Remote sensing techniques: A case of Koga watershed, Northwestern Ethiopia. *International Soil and Water Conservation Research*, 4(2), 126-136.
- Gerssen-Gondelach, S. J., Lauwerijssen, R. B., Havlík, P., Herrero, M., Valin, H., Faaij, A. P., & Wicke, B. (2017). Intensification pathways for beef and dairy cattle production systems: Impacts on GHG emissions, land occupation and land use change. *Agriculture, Ecosystems & Environment*, 240, 135-147.
- Green, K., Congalton, R. G., & Tukman, M. (2017). *Imagery and GIS: best practices for extracting information from imagery* (Vol. 1). Esri Press Redlands, CA.
- Gunawan, G., Sutjiningsih, D., Soeryantono, H., & Widjanarko, S. (2013). Soil Erosion Prediction Using GIS and Remote Sensing on Manjuntio Watershed Bengkulu, Indonesia. *Journal of Tropical Soils*, 18(2), 141-148.
- Halmy, M. W. A., Gessler, P. E., Hicke, J. A., & Salem, B. B. (2015). Land use/land cover change detection and prediction in the north-western coastal desert of Egypt using Markov-CA. *Applied Geography*, 63, 101-112.
- Hansen, M. C., Potapov, P. V., Moore, R., Hancher, M., Turubanova, S. A., Tyukavina, A., Thau, D., Stehman, S. V., Goetz, S. J., & Loveland, T. R. (2013). High-resolution global maps of 21st-century forest cover change. *Science*, 342(6160), 850-853.
- Hassan, F. A. (1979). Geoarchaeology: The geologist and archaeology. *American Antiquity*, 44(2), 267-270.
- Hassan, Z., & Arshad, M. (2006). Land Degradation in Pakistan: A Serious Threat to Environments and Economic Sustainability. *Editorial, Green Pages*.
- Haygarth, P. M., & Ritz, K. (2009). The future of soils and land use in the UK: soil systems for the provision of land-based ecosystem services. *Land use policy*, 26, S187-S197.
- He, X., Xu, Y., & Zhang, X. (2007). Traditional farming system for soil conservation on slope farmland in southwestern China. *Soil and Tillage Research*, 94(1), 193-200.
- Hudson, N. W. (1965). *The influence of rainfall on the mechanics of soil erosion: with particular reference to Southern Rhodesia* [University of Cape Town].
- IPCC, C. C. (2007). The physical science basis. Contribution of working group I to the fourth assessment report of the Intergovernmental Panel on Climate Change. *Cambridge University Press, Cambridge, United Kingdom and New York, NY, USA*, 996(2007), 113-119.
- Jie, C., Jing-Zhang, C., Man-Zhi, T., & Zi-tong, G. (2002). Soil degradation: a global problem endangering sustainable development. *Journal of Geographical Sciences*, 12, 243-252.
- Kalnay, E., & Cai, M. (2003). Impact of urbanization and land-use change on climate. *Nature*, 423(6939), 528-531.
- Kassa, H., Dondeyne, S., Poesen, J., Frankl, A., & Nyssen, J. (2017). Impact of deforestation on soil fertility, soil carbon and nitrogen stocks: the case of the Gacheb catchment in the White Nile Basin, Ethiopia. *Agriculture, Ecosystems & Environment*, 247, 273-282.
- Khan, A., Ahmad, D., & Shah Hashmi, H. (2013). *Review of available knowledge on land degradation in Pakistan*.

- Kiprotich, P., Wei, X., Zhang, Z., Ngigi, T., Qiu, F., & Wang, L. (2021). Assessing the impact of land use and climate change on surface runoff response using gridded observations and swat+. *Hydrology*, 8(1), 48.
- Kirkby, M. (1976). Tests of the random network model, and its application to basin hydrology. *Earth Surface Processes*, 1(3), 197-212.
- Koch, M., Bowes, G., Ross, C., & Zhang, X. H. (2013). Climate change and ocean acidification effects on seagrasses and marine macroalgae. *Global change biology*, 19(1), 103-132.
- Kocuyigit, R., & Demirci, S. (2012). Long-term changes of aggregate-associated and labile soil organic carbon and nitrogen after conversion from forest to grassland and cropland in northern Turkey. *Land Degradation & Development*, 23(5), 475-482.
- Kurothe, R., Kumar, G., Singh, R., Singh, H., Tiwari, S., Vishwakarma, A., Sena, D., & Pande, V. (2014). Effect of tillage and cropping systems on runoff, soil loss and crop yields under semiarid rainfed agriculture in India. *Soil and Tillage Research*, 140, 126-134.
- Lal, R. (1988). Soil degradation and the future of agriculture in sub-Saharan Africa. *Journal of soil and water conservation*, 43(6), 444-451.
- Lal, R. (1990). Soil erosion and land degradation: the global risks. *Advances in Soil Science: Soil Degradation Volume 11*, 129-172.
- Lal, R. (2001). Soil degradation by erosion. *Land Degradation & Development*, 12(6), 519-539.
- Lal, R. (2005). Soil erosion and carbon dynamics. In (Vol. 81, pp. 137-142): Elsevier.
- Lamb, D., Erskine, P. D., & Parrotta, J. A. (2005). Restoration of degraded tropical forest landscapes. *Science*, 310(5754), 1628-1632.
- Lambin, E. F., & Meyfroidt, P. (2011). Global land use change, economic globalization, and the looming land scarcity. *Proceedings of the National Academy of Sciences*, 108(9), 3465-3472.
- Landis, J. R., & Koch, G. G. (1977). An application of hierarchical kappa-type statistics in the assessment of majority agreement among multiple observers. *Biometrics*, 363-374.
- Livesley, S., Baudinette, B., & Glover, D. (2014). Rainfall interception and stem flow by eucalypt street trees—The impacts of canopy density and bark type. *Urban Forestry & Urban Greening*, 13(1), 192-197.
- Llerena-Montoya, S., Velastegui-Montoya, A., Zhirzhan-Azanza, B., Herrera-Matamoros, V., Adami, M., de Lima, A., Moscoso-Silva, F., & Encalada, L. (2021). Multitemporal analysis of land use and land cover within an oil block in the Ecuadorian Amazon. *ISPRS International Journal of Geo-Information*, 10(3), 191.
- Mena, C. F., Walsh, S. J., Frizzelle, B. G., Xiaozheng, Y., & Malanson, G. P. (2011). Land use change on household farms in the Ecuadorian Amazon: Design and implementation of an agent-based model. *Applied Geography*, 31(1), 210-222.
- Monserud, R. A., & Leemans, R. (1992). Comparing global vegetation maps with the Kappa statistic. *Ecological modelling*, 62(4), 275-293.
- Montgomery, D. R. (2007). Soil erosion and agricultural sustainability. *Proceedings of the National Academy of Sciences*, 104(33), 13268-13272.

- Morgan, R. (2001). A simple approach to soil loss prediction: a revised Morgan–Morgan–Finney model. *Catena*, 44(4), 305-322.
- Morgan, R., Morgan, D., & Finney, H. (1984). A predictive model for the assessment of soil erosion risk. *Journal of agricultural engineering research*, 30, 245-253.
- Morgan, R., Quinton, J., Smith, R., Govers, G., Poesen, J., Auerswald, K., Chisci, G., Torri, D., & Styczen, M. (1998). The European Soil Erosion Model (EUROSEM): a dynamic approach for predicting sediment transport from fields and small catchments. *Earth Surface Processes and Landforms: The Journal of the British Geomorphological Group*, 23(6), 527-544.
- Nabhan, H. (1999). Land degradation in relation to food security with focus on soil fertility management. *Integrated soil management for sustainable agriculture and food security in southern and east Africa*. Rome: FAO, 91-120.
- Nazif, W., Perveen, S., & Saleem, I. (2006). Status of micronutrients in soils of district Bhimber (Azad Jammu and Kashmir). *Journal of Agricultural and Biological Science*, 1(2), 35-40.
- Nearing, M. A., Foster, G. R., Lane, L., & Finkner, S. (1989). A process-based soil erosion model for USDA-Water Erosion Prediction Project technology. *Transactions of the ASAE*, 32(5), 1587-1593.
- Owji, M. R., Nikkami, D., Mahdian, M. H., & Mahmoudi, S. (2012). Land use management in order to maximizing benefit and minimizing soil erosion. *International Journal of Soil Science*, 7(4), 157.
- Panagos, P., Borrelli, P., Meusburger, K., Alewell, C., Lugato, E., & Montanarella, L. (2015). Estimating the soil erosion cover-management factor at the European scale. *Land use policy*, 48, 38-50.
- Panagos, P., Meusburger, K., Ballabio, C., Borrelli, P., & Alewell, C. (2014). Soil erodibility in Europe: A high-resolution dataset based on LUCAS. *Science of the total environment*, 479, 189-200.
- Parveen, R., & Kumar, U. (2012). Integrated approach of universal soil loss equation (USLE) and geographical information system (GIS) for soil loss risk assessment in Upper South Koel Basin, Jharkhand.
- Pimentel, D., & Burgess, M. (2013). Soil erosion threatens food production. *Agriculture*, 3(3), 443-463.
- Pimentel, D., Harvey, C., Resosudarmo, P., Sinclair, K., Kurz, D., McNair, M., Crist, S., Shpritz, L., Fitton, L., & Saffouri, R. (1995). Environmental and economic costs of soil erosion and conservation benefits. *Science*, 267(5201), 1117-1123. <https://doi.org/10.1126/science.267.5201.1117>
- Quansah, C. (1982). *Laboratory experimentation for the statistical derivation of equations for soil erosion modelling and soil conservation design* [Cranfield Institute of Technology].
- Renard, Y. (1991). Institutional challenges for community-based management in the Caribbean. *Nature and Resources*, 27(4), 4-9.
- Reusing, M., Schneider, T., & Ammer, U. (2000). Modelling soil loss rates in the Ethiopian Highlands by integration of high resolution MOMS-02/D2-stereo-data in a GIS. *International Journal of remote sensing*, 21(9), 1885-1896.
- Rosewell, C. J. (1986). Rainfall kinetic energy in eastern Australia. *Journal of Applied Meteorology and Climatology*, 25(11), 1695-1701.

- Sahu, R., Rawat, A., & Rao, D. (2015). Traditional rainwater management system ('Haveli') in vertisols of central India improves carbon sequestration and biological soil fertility. *Agriculture, Ecosystems & Environment*, 200, 94-101.
- Saravanan, S., Saranya, T., Abijith, D., Jacinth, J. J., & Singh, L. (2021). Delineation of groundwater potential zones for Arkavathi sub-watershed, Karnataka, India using remote sensing and GIS. *Environmental Challenges*, 5, 100380.
- Sayyad, A. M., Suleiman, Y., & Mairo, M. (2019). Impact of Deforestation on Land Degradation in Shiroro Local Government Area, Niger State Nigeria.
- Searchinger, T. D., Wiersenius, S., Beringer, T., & Dumas, P. (2018). Assessing the efficiency of changes in land use for mitigating climate change. *Nature*, 564(7735), 249-253.
- Sepuru, T. K., & Dube, T. (2018). An appraisal on the progress of remote sensing applications in soil erosion mapping and monitoring. *Remote Sensing Applications: Society and Environment*, 9, 1-9.
- Serpa, D., Nunes, J., Santos, J., Sampaio, E., Jacinto, R., Veiga, S., Lima, J., Moreira, M., Corte-Real, J., & Keizer, J. (2015). Impacts of climate and land use changes on the hydrological and erosion processes of two contrasting Mediterranean catchments. *Science of the total environment*, 538, 64-77.
- Shah, F., & Wu, W. (2019). Soil and crop management strategies to ensure higher crop productivity within sustainable environments. *Sustainability*, 11(5), 1485.
- Siddiqui, S., Safi, M. W. A., Tariq, A., Rehman, N. U., & Haider, S. W. (2020). GIS based universal soil erosion estimation in District Chakwal Punjab, Pakistan. *International Journal of Economic and Environmental Geology*, 11(2), 30-36.
- Sinha, D., & Joshi, V. U. (2012). Application of universal soil loss equation (USLE) to recently reclaimed badlands along the Adula and Mahalungi Rivers, Pravara Basin, Maharashtra. *Journal of the Geological Society of India*, 80, 341-350.
- Solaimani, K., Modallaldoust, S., & Lotfi, S. (2009). Investigation of land use changes on soil erosion process using geographical information system. *International Journal of Environmental Science & Technology*, 6, 415-424.
- Sonneveld, B., & Keyzer, M. (2003). Land under pressure: soil conservation concerns and opportunities for Ethiopia. *Land Degradation & Development*, 14(1), 5-23.
- Tarariko, O., Iliencko, T., Kuchma, T., & Novakovska, I. (2019). Satellite agroecological monitoring within the system of sustainable environmental management.
- Tariq, A., Riaz, I., Ahmad, Z., Yang, B., Amin, M., Kausar, R., Andleeb, S., Farooqi, M. A., & Rafiq, M. (2020). Land surface temperature relation with normalized satellite indices for the estimation of spatio-temporal trends in temperature among various land use land cover classes of an arid Potohar region using Landsat data. *Environmental Earth Sciences*, 79, 1-15.
- Thompson, A., Gantzer, C., & Anderson, S. (1991). Topsoil depth, fertility, water management, and weather influences on yield. *Soil Science Society of America Journal*, 55(4), 1085-1091.
- Tiwari, A., Risse, L., & Nearing, M. (2000). Evaluation of WEPP and its comparison with USLE and RUSLE. *Transactions of the ASAE*, 43(5), 1129-1135.
- Towers, W., Grieve, I., Hudsonm, G., Campbell, C., Lilly, A., Davidson, D., Bacon, J., Langan, S., & Hopkins, D. (2006). Report on the current state and threats to Scotland's soil resource. *Environmental Research Report*, 1.

- Turner, B. L., Lambin, E. F., & Reenberg, A. (2007). The emergence of land change science for global environmental change and sustainability. *Proceedings of the National Academy of Sciences*, 104(52), 20666-20671.
- Van Oost, K., Quine, T., Govers, G., De Gryze, S., Six, J., Harden, J., Ritchie, J., McCarty, G., Heckrath, G., & Kosmas, C. (2007). The impact of agricultural soil erosion on the global carbon cycle. *Science*, 318(5850), 626-629.
- Vishnudas, S. (2006). *Sustainable Watershed Management: Illusion or Reality?* Eburon Uitgeverij BV.
- Wang, C., & Yang, Y. (2012). An overview of farmers' livelihood strategy change and its effect on land use/cover change in developing countries. *Progress in Geography*, 31(6), 792-798.
- Wilkinson, B. H., & McElroy, B. J. (2007). The impact of humans on continental erosion and sedimentation. *Geological society of America bulletin*, 119(1-2), 140-156.
- Wischmeier, W. H., & Smith, D. D. (1958). Rainfall energy and its relationship to soil loss. *Eos, Transactions American Geophysical Union*, 39(2), 285-291.
- Wischmeier, W. H., & Smith, D. D. (1978). *Predicting rainfall erosion losses: a guide to conservation planning*. Department of Agriculture, Science and Education Administration.
- Zanchi, C., & Torri, D. (1980). Evaluation of rainfall energy in central Italy. *Evaluation of rainfall energy in central Italy.*, 133-142.